	ESA Contract:	1/6287/11/I-NB
		Doc. Title	D5000 Impact Assessment
		Doc. No	Report NCL_CRUCIAL_D5000
		Version No	2
		Date	06.04.17



**CryoSat-2 sUccess over Inland water And Land (CRUCIAL) Contract  
1/6287/11/I-NB**

**D5000 Impact Assessment Report (IAR)**

Document No: **NCL\_CRUCIAL\_D5000**

Issue: **2**

Issue Date: **6 April 2017**

		ESA Contract:	1/6287/11/I-NB
		Doc. Title	D5000 Impact Assessment Report
		Doc. No	NCL_CRUCIAL_D5000
Version No	2	Date	06.04.17

Author (Chapters 1-4): Philip Moore

Signature: 

Author (Chapter 5): Steve Birkinshaw

Signature: 

Author (Chapter 6): Peter Bauer-Gottwein



Signature: 

Author (Chapter 6): Raphael Schneider

Signature: 



Authorised by: Philip Moore

Signature: 

		ESA Contract:	1/6287/11/I-NB
		Doc. Title	D5000 Impact Assessment
		Doc. No	Report NCL_CRUCIAL_D5000
		Version No	2
		Date	06.04.17



### Document Change Record

Version	Date	Modified by	Description
1	06.12.16	PM, PB-G	Created
2	06.04.17	PM	Amendments based on ESA recommendations

		ESA Contract:	1/6287/11/I-NB
		Doc. Title	D5000 Impact Assessment
		Doc. No	Report NCL_CRUCIAL_D5000
		Version No	2
		Date	06.04.17



## Abstract

This document summarises the impact and benefits of the CryoSat-2 data in the context of inland water applications from SAR FBR and SARin FBR data. Quantification of the errors/uncertainties are attempted along with the improvements provided by the product. The potential impact of the product to enhance the current state-of-the-art knowledge is assessed. The experimental datasets from the methodologies of D4100, Algorithm Theoretical Basis Report (ATBD), and D4200, the Product Validation Report (PVR), are compared against in-situ measurements and existing datasets to provide an estimate as to the accuracy of the measurement. In particular, heights from SAR/SARin inland water products are compared against in-situ gauge measurements and contemporaneous altimeter heights from Jason-2 where possible, with the CryoSat-2 inland water measurements placed in context with those from prior missions. The ESA CRUCIAL project has been one of the first attempts to systematically explore and exploit the value of CryoSat-2 altimetry data for river analysis and data assimilation in hydrologic modeling. The project has generated new knowledge and insight that can support future applications of the mission over rivers.



		ESA Contract:	1/6287/11/I-NB
		Doc. Title	D5000 Impact Assessment
		Doc. No	Report NCL_CRUCIAL_D5000
		Version No	2
		Date	06.04.17

## Contents

<b>Abstract.....</b>	<b>4</b>
<b>Figures.....</b>	<b>7</b>
<b>Tables.....</b>	<b>10</b>
<b>1 Introduction .....</b>	<b>11</b>
<b>1.1 Abbreviations and Acronyms .....</b>	<b>11</b>
<b>1.2 Purpose and Scope .....</b>	<b>13</b>
<b>1.3 Inland Water Studies .....</b>	<b>13</b>
<b>2 SAR/SARin waveforms from L1A data.....</b>	<b>15</b>
<b>2.1 Multi-look Analysis.....</b>	<b>15</b>
<b>2.2 G-POD SARvatore and SARinvatore .....</b>	<b>16</b>
<b>2.3 SARin analyses of cross angle.....</b>	<b>17</b>
<b>3 FBR Product and Validation.....</b>	<b>17</b>
<b>3.1 Tonlé Sap .....</b>	<b>18</b>
<b>3.2 Mekong.....</b>	<b>24</b>
<b>3.3 Amazon.....</b>	<b>33</b>
<b>4 SARin FBR Product and Validation .....</b>	<b>40</b>
<b>4.1 Amazon.....</b>	<b>40</b>
4.1.1 SARin Heights .....	40
4.1.2 Validation against gauge data at Tabatinga calibration.....	40
4.1.3 Analysis of the cross angle near the Tabatinga gauge .....	44
<b>4.2 Brahmaputra .....</b>	<b>49</b>
<b>5 Summary of validation of FBR SAR and SARin inland water heights .....</b>	<b>52</b>
<b>6 Informing regional-scale hydrodynamic models with CryoSat-2 Altimetry .....</b>	<b>55</b>
<b>6.1 Implications of the orbit configuration for hydrologic analysis .....</b>	<b>56</b>
<b>6.2 Preprocessing of CryoSat-2 altimetry.....</b>	<b>57</b>

		ESA Contract:	1/6287/11/I-NB
		Doc. Title	D5000 Impact Assessment
		Doc. No	Report NCL_CRUCIAL_D5000
		Version No	2
		Date	06.04.17

<b>6.3 Calibration of river morphology parameters.....</b>	<b>59</b>
<b>6.4 Synthetic assimilation experiments.....</b>	<b>61</b>
<b>6.5 Assimilation of real CryoSat-2 altimetry .....</b>	<b>63</b>
<b>6.6 Summary and conclusions.....</b>	<b>65</b>
<b>7. References.....</b>	<b>66</b>

		ESA Contract:	1/6287/11/I-NB
		Doc. Title	D5000 Impact Assessment
		Doc. No	Report NCL_CRUCIAL_D5000
		Version No	2
		Date	06.04.17

## Figures

Figure 1: Pass across Tonlé Sap of 3 Dec 2011. 80 Hz burst data (black); running average over 4 points of burst data (blue) and multi-look with N=40 (red). The orthometric height is the height on the surface above the EGM96 geoid. ....	16
Figure 2: Google earth image of Tonlé Sap. The locations of the 62 CryoSat-2 heights are given by the yellow circles. The location of the two gauges are indicated by turquoise markers. The position of the S-N OSTM altimetric pass is given by the red marker. ....	21
Figure 3: Time series of aligned heights across Tonlé Sap. OSTM black points, CryoSat-2 red and Prek Kdam gauge heights blue points. ....	22
Figure 4: Location of 5 gauges along the Mekong, the Khone Phapheng Falls and the 0 km chainage point of Figure 5. ....	25
Figure 5: SAR FBR heights along the Mekong (N=40). Gauges and range identified by lines/circles. Circles at gauge show low water level (Dec-Apr) and high water level (Aug-Sep). Gauges at Mukdahan, Khong Chiam, Pakse, Stung Teng, Kratie ordered from low to high chainage. Low water level (Dec-Apr). High water level Waterfall located at chainage 620km. The 0 km chainage location corresponds to (18.23536°N, 104.0412°E). ....	27
Figure 6: Google earth image overlaid by CryoSat-2 passes across the Mekong near the Kratie gauge (red circle) and the two ENVISAT/Altika crossing points ....	31
Figure 7: Comparison of Kratie gauge data with heights from near-by altimetric points from NCL (this study) waveforms using N=40. RMS 67.8 cm (empirical retracers) and 66.9 cm (OCOG/Threshold) using 3 $\sigma$ rejection level. ....	32
Figure 8: Differences between gauge heights at Kratie and the CryoSat-2 heights modified for river slope (courtesy of Mekong River Commission). ....	33
Figure 9: Google earth image overlaid by CryoSat-2 passes across the Amazon near the Obodos gauge (red circle) and the two ENVISAT/Altika crossing points ....	36
Figure 10: Google earth image overlaid by CryoSat-2 passes across the Amazon near the Manacapuru gauge (red circle) and the two ENVISAT/Altika crossing points. ....	37
Figure 11: FBR SAR heights (N=40, empirical retracers) at Obidos using both a 2.5 $\sigma$ rejection level and slope adjustment (RMS 27.3 cm). ....	38
Figure 12: FBR SAR heights (N=40, empirical retracers) at Manacapuru using both a 3 $\sigma$ rejection level and slope adjustment (RMS 53.6 cm). ....	39



		ESA Contract:	1/6287/11/I-NB
		Doc. Title	D5000 Impact Assessment
		Doc. No	Report NCL_CRUCIAL_D5000
		Version No	2
		Date	06.04.17

Figure 13: Google earth image of Amazon near Tabatinga; gauge marked as red circle with ..... 42

Figure 14: Tabatinga gauge heights and CryoSat-2 SARin (N=60, OCOG/Threshold) heights corrected for river slope. RMS difference 29.9 cm. .... 43

Figure 15: Plot of the 64 accepted cross angles comprising 44 ascending passes (black squares) and 20 descending passes (red squares). .... 43

Figure 16: SARin waveforms (upper), coherence (middle) and cross angle in degrees (lower). In the upper plot the right antennae is coloured blue and the left antennae is green. X-axis is bin number; Y axis is power (upper), coherence (middle) and degree (lower). Left hand column location #274 (3.930 °S 70.207 °W); right hand column location #275 (3.927 °S 70.207 °W). Date of pass 5 May 2012. .... 46

Figure 17: OCOG/Threshold based difference between heights from the two SARin antennae (Upper). Cross angle (Lower). SARin Amazonas 5 May 2012. (Latitude -4.2° corresponds to longitude 70.179°W). .... 47

Figure 18: Google earth plot of descending pass on 8 September 2012 across Amazon near Tabatinga (upper). Cross angles from SARin mode (lower). The blue arrow points along direction of flight. .... 48

Figure 19: CryoSat-2 SARin heights across the Brahmaputra. CRUCIAL heights (N=60, OCOG/THreshold) (black squares) and DTU derived heights (red squares). .... 50

Figure 20: The height difference between NCL and DTU heights across the Brahmaputra. Accepted points denoted by black squares, rejected points by red squares. Mean difference and standard deviation of accepted points 11.9cm and 15.8 cm, respectively. 51

Figure 21: CryoSat-2 sampling pattern over the Brahmaputra in the Assam Valley for the year 2012 ..... 57

Figure 22: Section of the Brahmaputra in the Assam valley showing the Landsat river mask, the CryoSat-2 observations and their mapping to the 1D river model, all for 2013. .... 58

Figure 23: Clustering of individual CryoSat-2 data points from one river crossing based on k-means clustering. The left panel shows a crossing from 09-04-2011, and the right panel from 30-10-2010. Note that the panels are showing different parts of the river, with the 2010 and 2011 river mask respectively. .... 59

Figure 24: Result of the river bottom elevation calibration for the Assam Valley for the period 2010 to 2013. All levels are shown relative to the reference model's cross section datums based on SRTM DEM. .... 60







		ESA Contract:	1/6287/11/I-NB
		Doc. Title	D5000 Impact Assessment
		Doc. No	Report NCL_CRUCIAL_D5000
		Version No	2
		Date	06.04.17

Figure 25: Result of the opening angle calibration for one virtual station. All levels are relative to the water levels at the time of the first Envisat observation. The orbit provides a 35 day repeat cycle. .... 61

Figure 26: Results of synthetic DA experiment with CryoSat-2 data ..... 62



Figure 27: Results of synthetic DA experiment with Sentinel-3A data ..... 62

Figure 28: Results of the DA of *real* CryoSat-2 data in terms of *discharge* at Bahadurabad station. The times of observations are marked with green dots on the x-axis. .... 64

		ESA Contract:	1/6287/11/I-NB
		Doc. Title	D5000 Impact Assessment
		Doc. No	Report NCL_CRUCIAL_D5000
		Version No	2
		Date	06.04.17

## Tables



Table 1: Statistics of fit for pass across Tonlé Sap 3 Dec 2011. G-POD: value from (indices 94:161) closest fit to CRUCIAL ground points in time; in parentheses values from indices 95-162. CRUCIAL values: top cosine weighting; lower unit weight. ....	20
Table 2: Time difference and auto-correlations between gauge data at Prek Kdam against the Kumong Luong gauge data and OSTM altimetric heights. ....	23
Table 3: RMS differences between gauge data at Prek Kdam advanced 12 days and OSTM and CryoSat-2 altimetric heights. ....	23
Table 4: Details of the 5 gauges along the Mekong including low water level, the high water level to low water level range, chainage from the upstream point corresponding to the northern limit of the SAR mask and the chainage range for the altimeter height comparisons. ....	26
Table 5: Mekong near Kratie: Comparisons of altimetric and gauge data. Chainage gives either extrema of distances from gauge or distance of crossing from gauge for a repeat orbit. Final column gives number of accepted measurements with rejected points in parenthesis. ....	30
Table 6: Comparison of altimetry against the Obidos gauge on the Amazon . Final column gives number of accepted measurements with rejected points in parenthesis. ....	35
Table 7: Statistics of cross track angles from the 64 passes near Tabatinga. The expected value of the slope from SARin height differences is $-0.0025^\circ$ . ....	44
Table 8: Results of DA experiments using real CryoSat-2 data. Performance is expressed in terms of discharge at Bahadurabad station. Sharpness is given as the width of the 90% confidence intervals.....	64

		ESA Contract:	1/6287/11/I-NB
		Doc. Title	D5000 Impact Assessment
		Doc. No	Report NCL_CRUCIAL_D5000
		Version No	2
		Date	06.04.17



## 1 Introduction

### 1.1 Abbreviations and Acronyms

Abbreviation	Meaning
ASTER	Advanced Spaceborne Thermal Emission and Reflection Radiometer
ATBD	Algorithm Theoretical Basis Document
CRPS	Continuous Ranked Probability Score
CRUCIAL	CryoSat-2 sUCcess over Inland water And Land
DA	Data Assimilation
DAHITI	Database for Hydrological Time Series of Inland Waters
DEM	Digital Elevation Model
DTU	Danish Technical University
EGM96	Earth Gravity Model 1996
EGM08	Earth Gravity Model 2008
ERS-1/2	European Remote Sensing satellite 1 (2)
Envisat	Environmental Satellite
ESA	European Space Agency
FBR	Full Bit Rate
FFT	Fast Fourier Transform
G-POD	ESA's Ground-Processing On Demand service
ICESat	Ice, Cloud, and land Elevation Satellite

		ESA Contract:	1/6287/11/I-NB
		Doc. Title	D5000 Impact Assessment
		Doc. No	Report NCL_CRUCIAL_D5000
		Version No Date	2 06.04.17

L1A	Level 1A
L1B	Level 1B
LRM	Low Resolution Mode
JASON	US/French Altimeter Satellite
NCL	Newcastle University
OCOG	Offset Centre of Gravity
OSTM	Ocean Surface Topography Mission (JASON-2)
PVR	Product Validation Report
RA	Radar Altimeter
RMS	Root Mean Square
R&L	River and Lake
SAMOSA	SAR Altimetry MOde Studies and Applications
SAR	Synthetic Aperture Radar mode of CryoSat-2 SIRAL
SARAL	Satellite with ARGos and ALtiKa
SARin	Interferometric Synthetic Aperture Radar mode of CryoSat-2 SIRAL
SARvatore	SARin Versatile Altimetric Toolkit for Ocean Research & Exploitation
SARinvatore	SARin Versatile Altimetric Toolkit for Ocean Research & Exploitation
Sentinel-3	ESA Earth Observation Satellite Mission
SIRAL	SAR Interferometric Radar Altimeter
SRTM	Shuttle Radar Topography Mission

		ESA Contract:	1/6287/11/I-NB
		Doc. Title	D5000 Impact Assessment
		Doc. No	Report NCL_CRUCIAL_D5000
		Version No	2
		Date	06.04.17



## 1.2 Purpose and Scope

CryoSat-2 was launched on 8 April 2010 following on from previous ESA Earth orbiting satellite radar altimeters (e.g. ERS2 and Envisat) that have been used for land surface applications including mapping and measurement of river and lake systems. CryoSat-2's primary instrument is SIRAL (SAR Interferometric Radar Altimeter), which uses radar pulses to determine and monitor the spacecraft's altitude. Although the CryoSat-2 primary aim is to measure sea ice and ice sheets it can provide valuable data over the rest of the Earth surface. SIRAL operates in one of three modes, depending on where (above the Earth's surface) CryoSat-2 is flying. The three modes are: the conventional altimeter mode or Low resolution Mode (LRM), the Synthetic Aperture Radar (SAR) mode and Interferometric Synthetic Aperture Radar (SARin) mode. CryoSat-2 is in a low non Sun-synchronous Earth orbit of period of 100 minutes. The orbit of CryoSat-2 drifts across the Earth's surface with a repeat cycle of 369 days.

CRUCIAL is investigating innovative land and water applications from CryoSat-2 with a forward-look component to the future Sentinel-3 mission. This document aims to analyze heights derived from waveforms utilizing the CryoSat-2 FBR L1A SAR/SARin data based on methodologies described in the Algorithm Theoretical Basis Document (ATBD, D4100) and the Product Validation Report (PVR, D4200). In particular this report utilizes comparisons of inland water heights from CryoSat-2 SAR and SARin L1A FBR data against in situ river gauge data and heights derived from the Jason-2 (OSTM) mission to draw conclusions as to the accuracy of SIRAL. Comparisons also refer to data from ESA's Ground-Processing on demand (G-POD) services SARvatore (**SAR Versatile Altimetric Toolkit for Ocean Research & Exploitation**) and SARinvatore (**SARin Versatile Altimetric Toolkit for Ocean Research & Exploitation**). CryoSat-2 heights across the Brahmaputra are assimilated and utilized in hydrodynamic modelling.

## 1.3 Inland Water Studies



All previous altimetric missions utilized standard LRM nadir pointing altimetry while the CryoSat-2 mission is the first to operate a SAR mode altimeter. With the exception of ERS-1 in its geodetic phase and now CryoSat-2 all previous altimeter missions have a repeat orbit in which the satellite follows the same ground-track after a number of days; 35 days for ERS-2 and Envisat and 10 days for Topex/Poseidon, Jason-1, Jason-2 (OSTM) and the recently launched Jason-3 (OSTM2). This presents an added difficulty for hydrological modelling as well as for the validation as the crossing points of inland waters migrate with the ground track.

		ESA Contract:	1/6287/11/I-NB
		Doc. Title	D5000 Impact Assessment
		Doc. No	Report NCL_CRUCIAL_D5000
		Version No	2
		Date	06.04.17

To place CryoSat-2 results into context we refer again to some previous studies.

Water heights from CryoSat-2 retracked Level 1B (L1B) SAR waveforms were compared against gauge levels from 5 lakes in Scandinavia (Nielsen et al., 2015). The authors utilize a static and a dynamic model, the latter using observations that are close in time. The dynamic model provides reliable heights even for noisy and sparse data while the static approach fails on occasions. A dynamic approach is viable over slowly fluctuating lake levels with multiple passes but cannot be transferred to a river with highly fluctuating water levels even at close time intervals because of the low degree of correlation between observations. The RMS values presented in that paper show agreement with gauge data at the 5-16 cm level for the larger lakes. The paper infers that for smaller lakes CryoSat-2 derived heights are of higher accuracy compared to Envisat heights.

Song et al. (2015a,b) used CryoSat-2 altimetry and ICESat data to investigate change in lakes levels over the Tibetan Plateau. The authors used Level 2 heights from SARin data. Comparisons against two gauges (Song et al., 2015a) for Tibetan lakes yielded an RMS value of 0.18 m for Namco and 0.28 m for Yamzhog Yumco. Over Lake Nasser, Kleinherenbrink et al. (2014) used retracked SARin L1B waveforms. A comparison against Jason-2 altimetric heights yielded an RMS of 0.30 m which was an enhancement over the 0.73 m RMS from Level 2 data. The level 2 retracker errors range from 0.23 m over tracks with hardly any waveform pollution to 0.75 m with waveform pollution. The authors defined waveform pollution to be where several peaks were present in the cross-correlation function, which results in multiple elevations. Their retracker improves these values to 0.13 m and 0.21 m respectively. A dominant error source of about 0.2 m is the water surface slope caused by wind conditions and/or geoid errors.

		ESA Contract:	1/6287/11/I-NB
		Doc. Title	D5000 Impact Assessment
		Doc. No	Report NCL_CRUCIAL_D5000
		Version No	2
		Date	06.04.17

## 2 SAR/SARin waveforms from L1A data

This section provides a quick overview of the SAR/SARin processing methodology. Full details are available in D4100.



### 2.1 Multi-look Analysis

In the SAR (SARin) mode the burst echoes at 80 (20) Hz are processed through the following steps

- Range FFT over 64 pulses in burst
- Beam formation and steering to nadir direction
- Form burst centre ground points from OCOG/Threshold retracker applied to nadir beam
- Form a sequence of ground points at beam angle using a coarse approximate steering
- Beam formation and steering to ground points
- Stack beams pointing at ground points
- Apply slant range correction, tracker range correction and Doppler range correction
- Height retrieval from empirical and OCOG/Threshold retracker.

The multi-look waveforms for both SAR and SARin mode are about 320 m along the ground track; that is a reduction of resolution of a factor four compared to the burst echo separation.

A pertinent question for inland water applications is whether the burst echoes can supply useful heights at the higher spatial and temporal resolution. As an illustration, Figure 1 shows the orthometric heights for the pass on 3 Dec 2011 across Tonlé Sap, Cambodia. The figure shows the burst echoes heights derived by using the OCOG/Threshold retracker. Also given are heights from the stack forming the multi-look. The burst echo heights are considerably noisier than the multi-look data. To provide comparability at about 300 m resolution, a running average over 4 burst echo heights is also plotted but this also shows that the burst echoes by themselves cannot provide the precision of the multi-look approach. The speckle in the burst echo data affects the

		ESA Contract:	1/6287/11/I-NB
		Doc. Title	D5000 Impact Assessment
		Doc. No	Report NCL_CRUCIAL_D5000
		Version No	2
		Date	06.04.17

recovered heights and only through stacking and forming multi-look waveforms can precise heights be recovered. Burst echo heights are output for all passes studied within this project with similar results.

Conclusion: Multi-looking is essential due to radar speckle in the burst echoes.

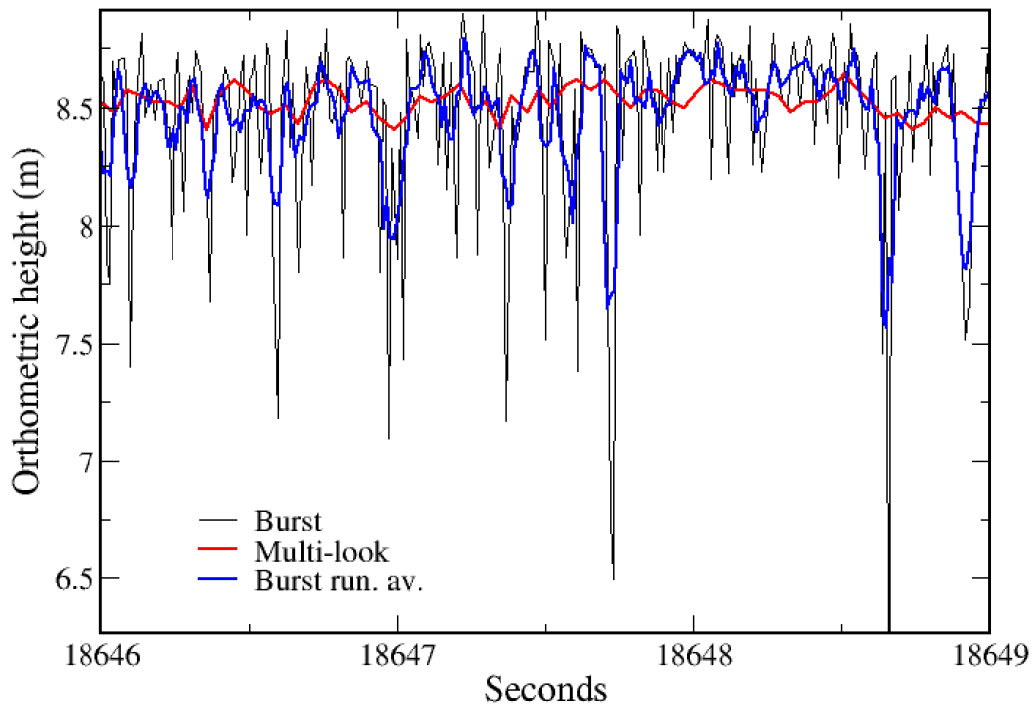




Figure 1: Pass across Tonlé Sap of 3 Dec 2011. 80 Hz burst data (black); running average over 4 points of burst data (blue) and multi-look with N=40 (red). The orthometric height is the height on the surface above the EGM96 geoid.

## 2.2 G-POD SARvatore and SARinvatore

Within this document, usage has been made of data downloaded from ESA's Ground-Processing on demand (G-POD) services SARvatore (**SAR** Versatile Altimetric Toolkit for **Ocean Research & Exploitation**) and SARinvatore (**SARin** Versatile Altimetric Toolkit for **Ocean Research &**



		ESA Contract:	1/6287/11/I-NB
		Doc. Title	D5000 Impact Assessment
		Doc. No	Report NCL_CRUCIAL_D5000
		Version No	2
		Date	06.04.17

Exploitation). The SARvatore service can be accessed by using the link [http://wiki.services.eoportal.org/tiki-index.php?page=GPOD+CryoSat-2+SARvatore+ Software + Prototype+ User+ Manual](http://wiki.services.eoportal.org/tiki-index.php?page=GPOD+CryoSat-2+SARvatore+Software+Prototype+User+Manual). Both SAR and SARin multi-look waveforms and heights derived by retracking with the SAMOSA2 retracker (Gommenginger et al., 2010) were downloaded. SARvatore and SARinvatore use all available waveforms in the stack to form the multi-look waveform. Note that the L2 products include the Stack Beam Index which gives the index of beams from 1 (minimum possible) to 260 (maximum possible) that have been summed to form the multi-look waveform.

Since the analyses were performed the SAMOSA+ retracker has become available on SARvatore/SARinvatore. SAMOSA+ is the SAMOSA2 model tailored for inland water, sea ice and coastal zone domain. This retracker needs consideration in future projects.

### 2.3 SARin analyses of cross angle



In SARin mode both antennae provide range measurements and the cross power between the two waveforms provides detail of the surface slope, as denoted by the angle  $\theta$ , over ice margins, etc. However, over inland waters the dominant reflectors can be from the water surface offset from nadir. Thus,  $\theta$  is now the sum of all water reflectors in the window and gives the cross angle of the reflectance; that is the angle of the summed reflectance of the water body from the nadir direction. The first returned signal will be from the water body closest to the nadir in the cross-track direction. If this body is substantial, this will form the leading edge for tracking.

The computations with the cross angle use the convention of left antennae minus right antennae. The phase difference will be positive if the target range using the left antennae exceeds that of the right antennae. Thus, conceptually for the satellite flying into the page, a positive cross track angle denotes a target to the right of the nadir point of the antennae center.

## 3 FBR Product and Validation

Within the context of this impact assessment a number of validation sites were utilized, namely:

1. Tonlé Sap river, Cambodia (SAR)
2. Mekong River (SAR)
3. Amazon (SAR)
4. Amazon (SARin)
5. Brahmaputra (SARin)

		ESA Contract:	1/6287/11/I-NB
		Doc. Title	D5000 Impact Assessment
		Doc. No	Report NCL_CRUCIAL_D5000
		Version No	2
		Date	06.04.17

### 3.1 Tonlé Sap

The Tonlé Sap river in Cambodia is selected as a primary validation site for FBR SAR data. Tonlé Sap is a relatively straightforward target as due to the expanse of water it can be considered a lake. Hydrologically, Tonlé Sap is a combined lake and river, in which the flow changes direction twice a year; the lake expanding and shrinking dramatically with the seasons. From November to May (dry season) Tonlé Sap drains into the Mekong River at Phnom Penh while after heavy rains (start June) Tonlé Sap backs up to form a lake.



Analyses in D4200 showed that multi-looking over a moderate number of waveforms in the stack is preferable. The preferred number of waveforms in the stack was parameterized by the number  $N$ , denoting the number of waveforms either side of the burst closest to nadir with the ground point in question. This gives a total  $2N+1$  waveforms used in the stack. D4200 and Table 1 show a preference for  $N \approx 40$ , rather than the maximum possible ( $N \approx 120$ ). The lower  $N$  gives a steeper leading edge to the multi-look waveform facilitating retracking. As the change in  $N$  causes an offset between the derived heights, which is indistinguishable from other contributions to the altimeter bias, a fixed value for  $N$  must be applied to all analyses to avoid bias. Also, in D4200 a Hamming window for weighting the waveforms was shown to outperform a unit weight (also see Table 1).

Conclusion: For SAR mode, a reduction in the number of waveforms in the stack to about 81 centred on the near nadir burst is preferred.

Conclusion: A weighting system based on the Hamming window is strongly recommended.

Data was additionally downloaded from ESA's G-POD Service using the SAMOSA2 retracker. Results in D4200 showed that the SAMOSA2 retracked heights are noisier than the CRUCIAL heights; this is caused by the SAMOSA2 retracker. To confirm this, the G-POD waveforms were retracked using the CRUCIAL empirical and OCOG/Threshold retrackers which significantly reduced the scatter in the derived heights as shown in Table 1. Note that retracking the G-POD waveforms gives greater variation in the heights than obtained with  $N=40$ .

All passes across Tonlé Sap (Figure 2) were analysed. Internal consistency of the heights for a particular pass provides a measure of the scatter in the data. Utilising the midline of Tonlé Sap all heights on either side were accepted until the multi-look waveform was best retracked by a double peak empirical retracker identifying reflectance off two water surfaces. This is not an



		ESA Contract:	1/6287/11/I-NB
		Doc. Title	D5000 Impact Assessment
		Doc. No	Report NCL_CRUCIAL_D5000
		Version No	2
		Date	06.04.17

infallible check on non-water surfaces as off nadir reflectors can dominate. To avoid utilizing such values in the low water height regime a maximum limit of 10 data points on either side of the midpoint was imposed in the first instance. Similarly, passes with 5 or less accepted data points were rejected. A total of 35 passes were analysed with RMS values between 2.44 cm and 13.6 cm; with mean  $4.62 \pm 0.19$  cm. This reduced to the range 2.44cm to 6.54 cm, with mean of  $4.35 \pm 0.10$  cm on eliminating one outlier. By increasing the number of possible points either side of the Tonlé Sap centre line from 10 to 20 gave a range 1.2 cm to 18.7 cm with mean  $6.0 \pm 3.4$  cm. There is risk now that in low flow regimes some points could be overland. However, we note that these values are still below or close to the minimum value of 5 cm found across the 5 lakes in Scandanavia by Nielsen et al. (2015) but without the need for any form of along track dynamic modelling.

Conclusion: Cryosat-2 SAR heights have precision of 4-6 cm on average.



For external validation, we used the OSTM, CryoSat-2 and Prek Kdam gauge heights when available as detailed in D4200. Using our approach the Prek Kdam time series is earlier than that of OSTM and CryoSat-2. A time correlation analysis by advancing the gauge data by an integral number of showed that a time advance of 11-13 days is optimal (Table 2). Utilising this advance an analysis of the differences between the gauge and altimetric heights shows that the 99 values of OSTM that overlap with the gauge data gave a RMS of 42.6 cm (Figure 3). For CryoSat-2 there are 26 values with RMS of 42.1 cm (see Table 3). Thus, there appears little difference between OSTM and CryoSat-2 heights for this test. It is noted that as the CryoSat-2 data is from non-repeating arcs we are reliant on the accuracy of the EGM08 geoid model to connect the ground tracks as well as the assumption that the time difference between the CryoSat-2 heights and the gauge data is the same 12 days as observed with OSTM. That this is not correct can be seen from the correlation analysis in Table 3 between the two gauges at Prek Kdam and Kumong Luong for the 8 years 2001-2009. For a location further north of the OSTM ground track such as Kumong Luong the time lapse compared to Prek Kdam is about 18.5 days. As the CryoSat-2 tracks cross Tonlé Sap in the main portion of the lake (see Figure 2) the use of 12 days is likely to be an underestimation.

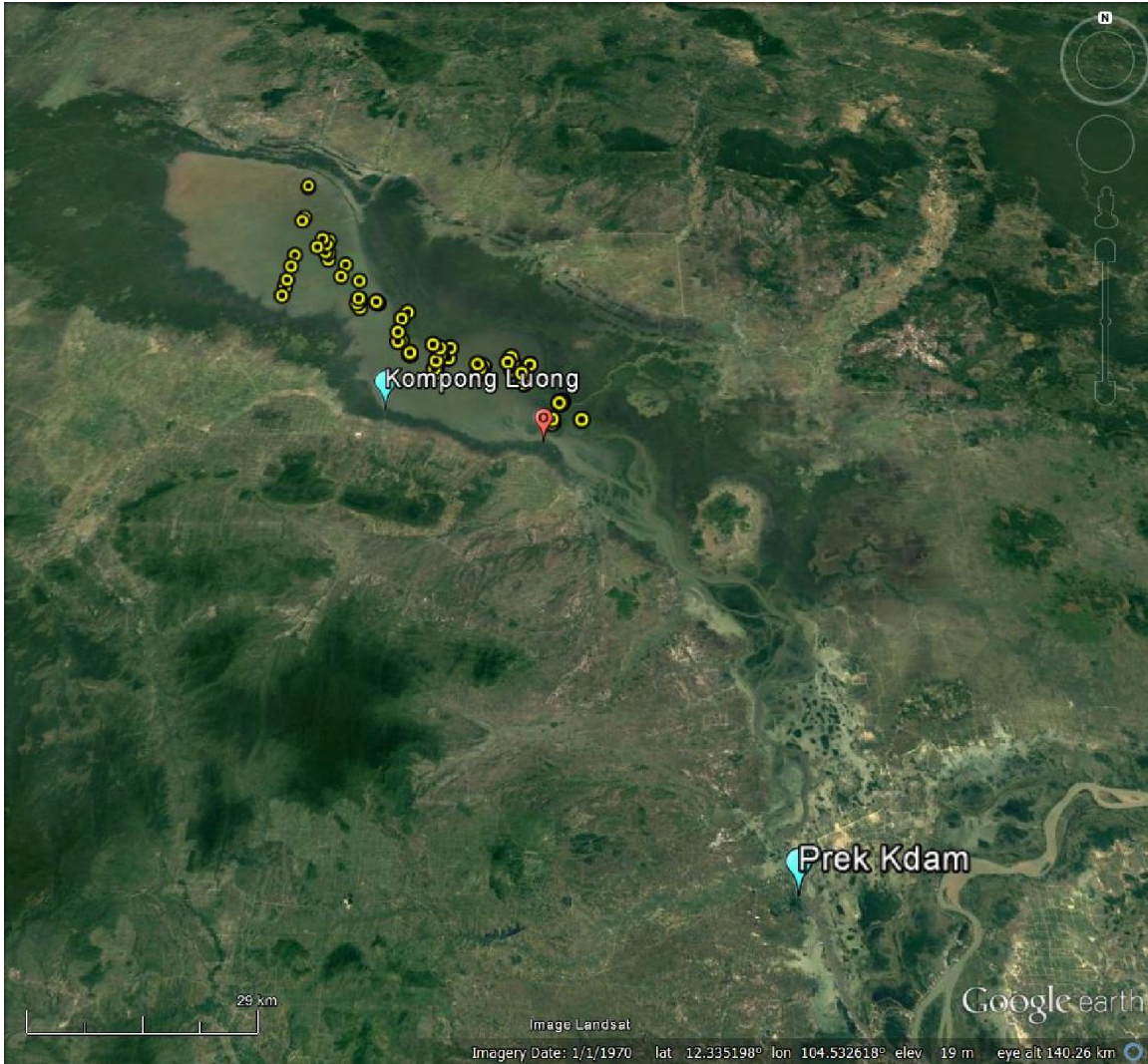
Conclusion: We cautiously infer that CryoSat-2 is performing better than OSTM across Tonlé Sap.

		ESA Contract:	1/6287/11/I-NB
		Doc. Title	D5000 Impact Assessment
		Doc. No	Report NCL_CRUCIAL_D5000
		Version No	2
		Date	06.04.17



Multi-look N	Sigma Empirical retrackers (cm)	Sigma OCO/Threshold (cm)
<b>G-POD: SAMOSA2</b>	7.39 (7.30)	
<b>G-POD: retracked</b>	5.88 (5.63)	7.18(6.60)
<b>140</b>	5.69	6.14
	6.01	6.23
<b>110</b>	5.72	6.08
	6.01	6.23
<b>90</b>	5.75	6.01
	6.01	6.23
<b>70</b>	5.58	5.81
	5.89	6.35
<b>40</b>	5.01	5.38
	5.87	5.88
<b>20</b>	5.20	5.09
	5.88	5.67
<b>10</b>	5.94	5.35
	5.74	5.03
<b>5</b>	9.20	7.66
	7.59	6.92

**Table 1: Statistics of fit for pass across Tonlé Sap 3 Dec 2011. G-POD: value from (indices 94:161) closest fit to CRUCIAL ground points in time; in parentheses values from indices 95-162. CRUCIAL values: top cosine weighting; lower unit weight.**

		ESA Contract:	1/6287/11/I-NB
		Doc. Title	D5000 Impact Assessment Report
		Doc. No	NCL_CRUCIAL_D5000
		Version No	2
		Date	06.04.17



**Figure 2: Google earth image of Tonlé Sap. The locations of the 62 CryoSat-2 heights are given by the yellow circles. The location of the two gauges are indicated by turquoise markers. The position of the S-N OSTM altimetric pass is given by the red marker.**

		ESA Contract:	1/6287/11/I-NB
		Doc. Title	D5000 Impact Assessment
		Doc. No	Report NCL_CRUCIAL_D5000
		Version No	2
		Date	06.04.17

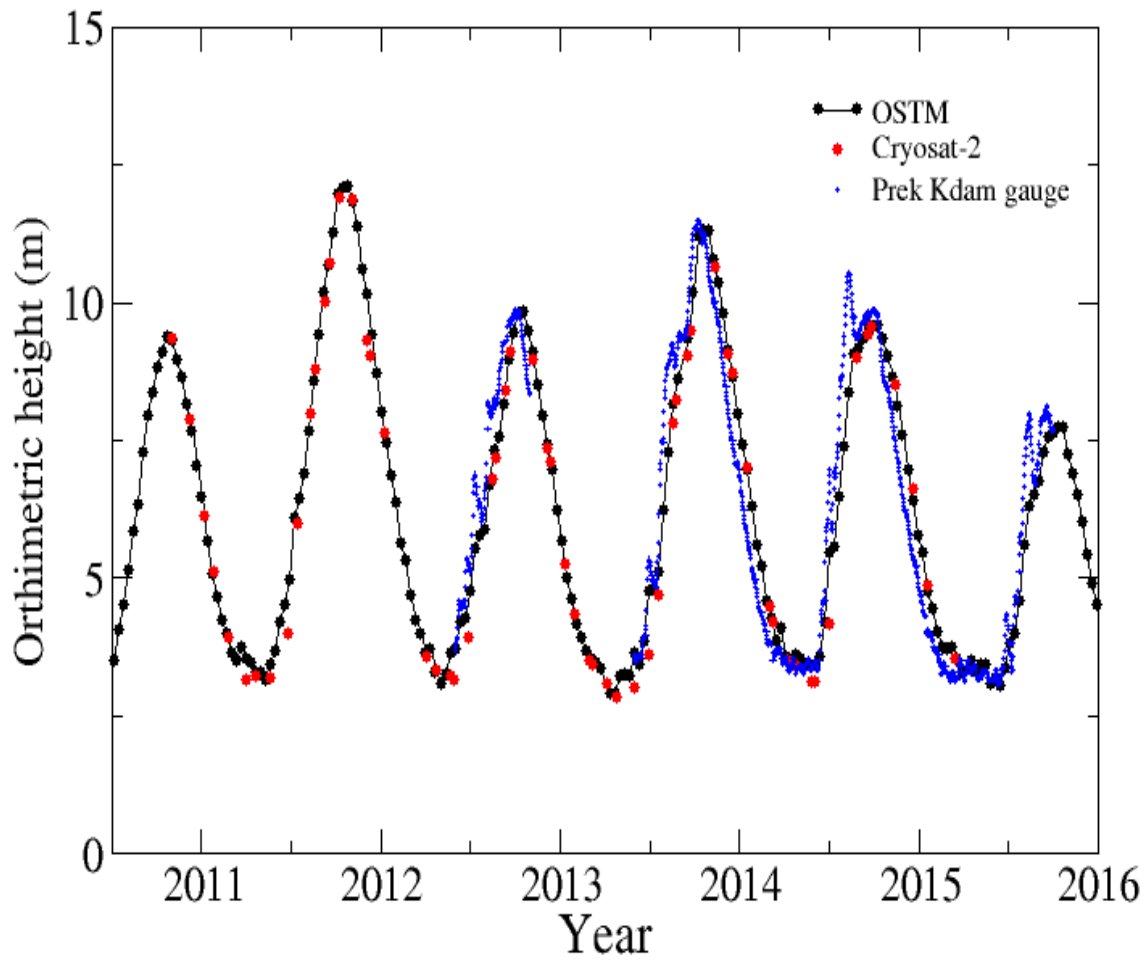




Figure 3: Time series of aligned heights across Tonlé Sap. OSTM black points, CryoSat-2 red and Prek Kdam gauge heights blue points.





		ESA Contract:	1/6287/11/I-NB
		Doc. Title	D5000 Impact Assessment
		Doc. No	Report NCL_CRUCIAL_D5000
		Version No	2
		Date	06.04.17

Prek Kdam days advanced	Correlation OSTM	Correlation Kumong Luong
0	0.962826	0.934639
6	0.982969	0.961042
11	0.988296	0.978429
12	0.988325	0.980823
13	0.987864	0.982860
17		0.987490
18		0.987807
19		0.987806
20		0.987491

**Table 2: Time difference and auto-correlations between gauge data at Prek Kdam against the Kumong Luong gauge data and OSTM altimetric heights.**

Satellite	#	RMS v Prek Kdam(t+12) (cm)
OSTM	99	42.6
CryoSat-2	26	42.1

**Table 3: RMS differences between gauge data at Prek Kdam advanced 12 days and OSTM and CryoSat-2 altimetric heights.**



		ESA Contract:	1/6287/11/I-NB
		Doc. Title	D5000 Impact Assessment
		Doc. No	Report NCL_CRUCIAL_D5000
		Version No	2
		Date	06.04.17

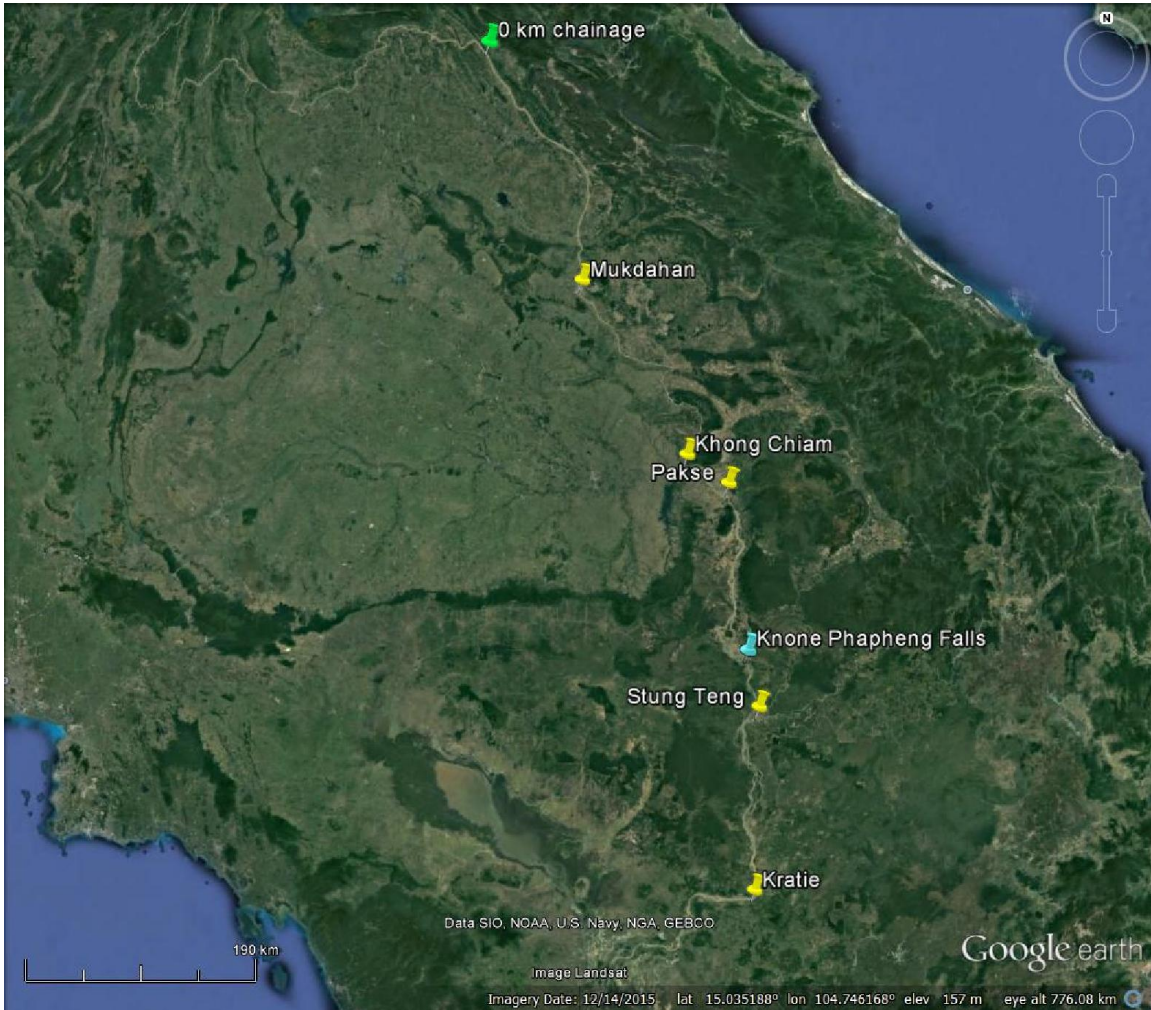
### 3.2 Mekong

All FBR SAR files for 16 Jul 2010 – 31 Mar 2015 were processed using the fine resolution Mekong river mask described in D4100. Again, as noted in D4200, the enhancement in the heights by replacing SAMOSA2 by the empirical retracers within the SARvatore waveform analysis is clearly evident. N=40 often gives an additional value over N=110, again confirming that a lower value of N is beneficial. It is not feasible to compare the two heights retracked from the CRUCIAL and SARvatore waveforms as ground points are offset and the solutions are sensitive to location.



Validation of CryoSat-2 heights across the Mekong has been undertaken by comparison against gauge data (Figure 4). We have access to data from five Mekong River gauges within the CryoSat-2 SAR collection area with the gauge details in Table 4. About 50 km upstream from Stung Teng, are the Khone Phapheng waterfalls. The falls are characterised by a series of rapids with thousands of islands stretching over about 10 km and with the highest fall of 21 m. The low water level made available by the Mekong River Commission is plotted in Figure 5. The chainage is measured from the upper boundary of the SAR recording area in the Mekong basin. The falls are seen at chainage 620 km.



		ESA Contract:	1/6287/11/I-NB
		Doc. Title	D5000 Impact Assessment Report
		Doc. No	NCL_CRUCIAL_D5000
		Version No	2
		Date	06.04.17





**Figure 4: Location of 5 gauges along the Mekong, the Khone Phapheng Falls and the 0 km chainage point of Figure 5.**

		ESA Contract:	1/6287/11/I-NB
		Doc. Title	D5000 Impact Assessment
		Doc. No	Report NCL_CRUCIAL_D5000
		Version No	2
		Date	06.04.17

#	Site	Latitude (deg)	Longitude (deg)	Low water level (m)	Range (m)	Chainage of gauge (km)	Chainage range altimetry (km)
013402	Mukdahan	16.540	104.737	124.5	11	222	158-321
013801	Khong Chiam	15.318	105.500	89.8	14	433	338-441
013901	Pakse	15.117	105.800	86.8	12	473	446-615
014501	Stung Teng	13.545	106.017	38.2	9	659	650-740
014901	Kratie	12.240	105.987	2.85	16	810	741-890

**Table 4: Details of the 5 gauges along the Mekong including low water level, the high water level to low water level range, chainage from the upstream point corresponding to the northern limit of the SAR mask and the chainage range for the altimeter height comparisons.**

		ESA Contract:	1/6287/11/I-NB
		Doc. Title	D5000 Impact Assessment Report
		Doc. No	NCL_CRUCIAL_D5000
		Version No	2
		Date	06.04.17

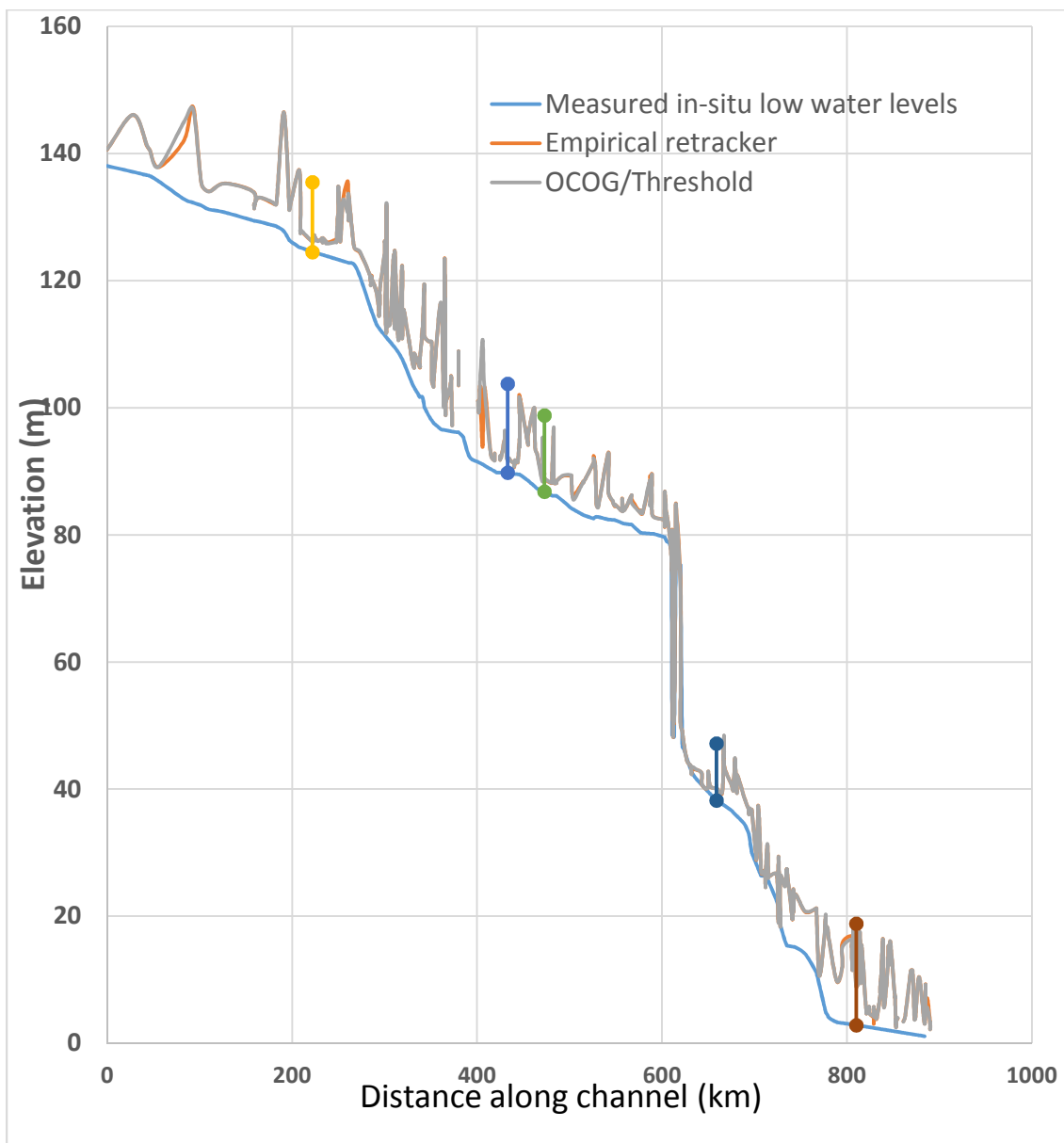


**Figure 5: SAR FBR heights along the Mekong (N=40). Gauges and range identified by lines/circles. Circles at gauge show low water level (Dec-Apr) and high water level (Aug-Sep). Gauges at Mukdahan, Khong Chiam, Pakse, Stung Teng, Kratie ordered from low to high chainage. Low water level (Dec-Apr). High water level Waterfall located at chainage 620km. The 0 km chainage location corresponds to (18.23536°N, 104.0412°E).**





		ESA Contract:	1/6287/11/I-NB
		Doc. Title	D5000 Impact Assessment
		Doc. No	Report NCL_CRUCIAL_D5000
		Version No	2
		Date	06.04.17

Figure 5 also shows the location of the 5 gauges along the Mekong with the circles denoting high (Aug-Sep) and low (Dec-Apr) flow levels. The low water levels at the gauges and the range are also given in Table 5. Table 5 also presents the chainage of each gauge from the 0 km chainage point (18.23536°N, 104.0412°E) and the chainage range for the altimeter height comparison. The zero chainage point corresponds to the northern limit of the CryoSat-2 SAR mode mask. All FBR SAR processed heights are plotted in Figure 5. Obvious outliers have been removed. Many of these are 10's of metres off the minimum level and represent unrealistic values. The outliers are identifiable without the low water level. These values are probably off ranging to water on high ground where the altimeter tracker is unable to follow the rapid change in topography from the highlands down to the river surface. This figure shows that the derived heights fall within the expected range near the gauge and also the spread of river locations that have been crossed by the satellite.

To quantify and validate the CryoSat-2 Mekong processing the heights were assigned to the nearest gauge to the Mekong crossing and subsequently corrected to the gauge location using the low water level slope. Such a correction will be less accurate at high water levels as the range is not consistent along the Mekong (Figure 5, Table 5). In addition to CRUCIAL derived heights, the Danish Technological University supplied their retracked heights based on the L1B waveforms. The RMS between the accepted DTU and NCL heights is 9.1 cm including values that are clearly off the Mekong.

Conclusion: The water heights from CRUCIAL and an independent retracking of SAR L1B waveforms is 9 cm RMS for the Mekong.

As shown in D4200 only data near Kratie (Figure 6) allows a detailed external investigation of the accuracy of altimetric data. The comparisons along the Mekong near Kratie between altimetric and gauge data (Figure 7) s summarized in Table 5 with the passes shown in Figure 6. The river width is constrained near Kratie being typically about 1900 m. DAHITI (Schwatke et al., 2015a) altimetric heights from the near identical ground tracks of ERS-2, Envisat and Alitka are available for two crossings 7 km and 43 km downstream from Kratie. Given the changing river morphology, the agreement between gauge and altimetry is expected to improve as the chainage between the locations is reduced (Figure 8). That the degree of fit of CryoSat-2 is not significantly worse than Envisat is a testament to CryoSat-2 as all other altimeter satellites were repeat pass while CryoSat-2 is non-repeating. The non-repeat orbit gives added complications from systematic errors due to the distance from Kratie and the different environs (e.g. width, islands, braiding) of the river crossings. Thus , for Envisat (Mar 2002 – Oct 2010) the RMS difference is 48.8 cm at 43 km chainage distance reducing to 42.9 cm at the 7 km chainage difference. SARAL/ Altika (Jun 2013 – Nov 2015) shows a greater improvement from 40.9 cm to 29.7 cm but the latter contains only 11 accepted measurements, with a further 4 rejected as



		ESA Contract:	1/6287/11/I-NB
		Doc. Title	D5000 Impact Assessment
		Doc. No	Report NCL_CRUCIAL_D5000
		Version No	2
		Date	06.04.17

outliers. Here, as in other comparisons, we rejected all differences at the  $3\sigma$  level. In contrast Birkinshaw et al (2010), using River&Lake data, found an RMS of 70.0 cm for ERS-2 and 65.0 cm for Envisat. In this study CryoSat-2 (chainage -5 to 80 km) gives an RMS of 59.9 cm. This value is dependent on the accuracy of the river slope correction. However, there is a signature evident in Figure 8 that is likely due to inaccuracies in this procedure. On utilizing a quadratic fit to the differences the RMS is reduced to 54.0 cm. Table 5 contains a number of chainage range for CryoSat-2 with, for example, an RMS of 50.5 cm for chainage range -5 to 26 km.

Note: Unlike previous altimeters the SARAL/AltiKa hardware is a single Ka band altimeter (35.75 GHz). The high frequency of the Ka band has several advantages over Ku band altimeters (Arsen et al., 2015) including a reduced antenna beam width, reduced radar footprint, increased Pulse Repetition Frequency (PRF), and better range resolution (0.47 m Envisat/CryoSat-2 etc, 0.3 m SARAL/AltiKa). In addition the Ka frequency is insensitive to the ionosphere thus removing the necessity of dual frequencies. Accordingly, the design is simpler and more lightweight. The disadvantage of the Ka band is its sensitivity to rain and clouds reducing the operational windows. Comparisons by Arsen et al. (2015) against in situ gauge data over mountain lakes in South America showed that SARAL/Altika gave greater coherence with the ground data and provided data significantly more accurate than Envisat. The authors showed that with Envisat the RMS accuracy ranged from 9 cm to several metres but only 5–17 cm for SARAL/AltiKa. In a later paper Schwatke et al. (2015b) showed that SARAL/Altika has the potential to decrease the RMS by about 10% for large lakes and 40% for selected rivers. Although only a few SARAL/Altika measurements are available to data the number rejected is about 30%. This may be indicative of problems with a Ka altimeter which is susceptible to cloud and rain in the footprint.

Conclusion: Comparison against gauge data is dependent on distance from gauge for a non-repeating orbit even if correction is made for river slope.



Conclusion: Given the conclusion about distance from gauge the CryoSat-2 comparisons are comparable to ENVISAT at Kratie on the Mekong but less accurate than SARAL/Altika

		ESA Contract:	1/6287/11/I-NB
		Doc. Title	D5000 Impact Assessment
		Doc. No	Report NCL_CRUCIAL_D5000
		Version No	2
		Date	06.04.17

Data Provider	Satellite	Period	Chainage (km)	RMS (cm)	#
<b>This study</b>	CryoSat-2		-5 to 6	43.7	13(1)
	CryoSat-2		-5 to 11	44.7	17(1)
	CryoSat-2		-5 to 26	50.5	28(1)
	CryoSat-2		-5 to 40	62.9	38(1)
	CryoSat-2		-5 to 50	64.1	47(2)
	CryoSat-2		-5 to 80	59.9	56(4)
<b>DAHITI</b>	Altika	Jun 2013 – Nov 2014	7	29.7	11(4)
	Altika		43	40.9	14(3)
	Envisat	Jul 2002 – Nov 2010	7	42.9	50(7)
	Envisat		43	48.8	34(3)
<b>River&amp;Lakes</b>	ERS-2	Apr 1995 – Jun 2003		70	
	Envisat	Jul 2002 – Mar 2006		65	



**Table 5: Mekong near Kratie: Comparisons of altimetric and gauge data. Chainage gives either extrema of distances from gauge or distance of crossing from gauge for a repeat orbit. Final column gives number of accepted measurements with rejected points in parenthesis.**

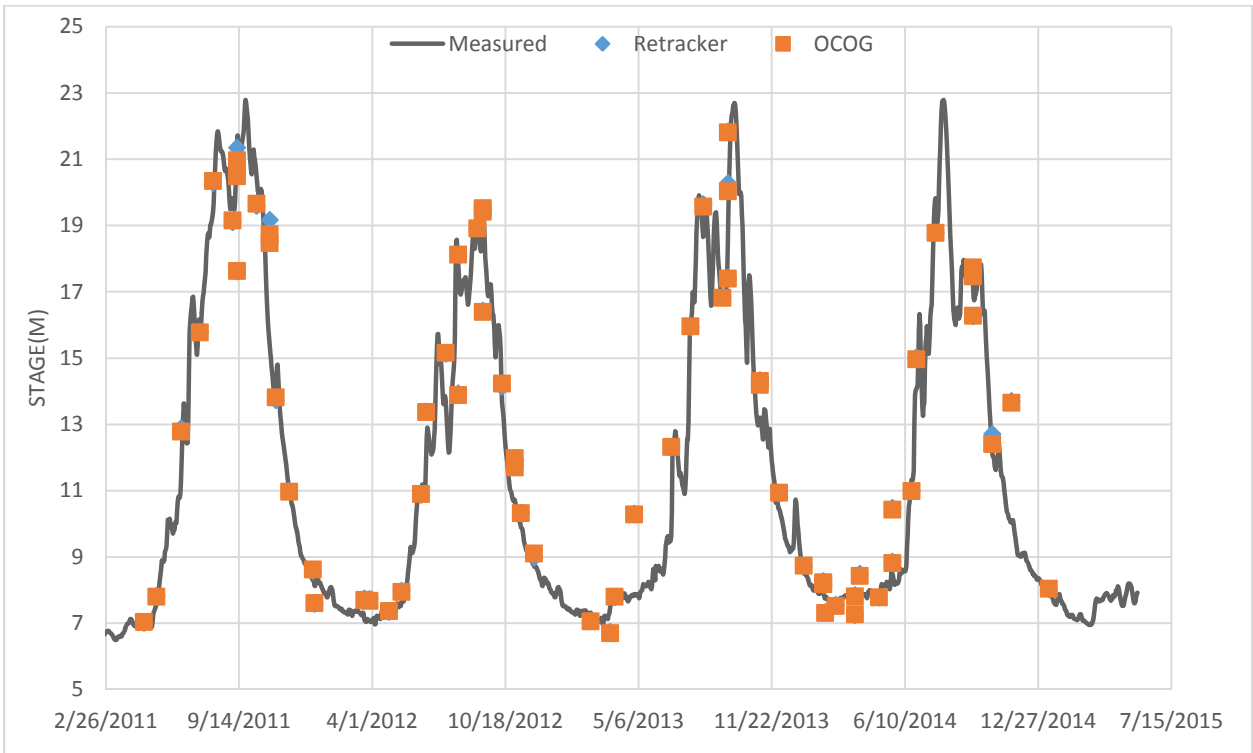


		ESA Contract:	1/6287/11/I-NB
		Doc. Title	D5000 Impact Assessment Report
		Doc. No	NCL_CRUCIAL_D5000
		Version No	2
		Date	06.04.17





**Figure 6: Google earth image overlaid by CryoSat-2 passes across the Mekong near the Kratie gauge (red circle) and the two ENVISAT/Altika crossing points**

		ESA Contract:	1/6287/11/I-NB
		Doc. Title	D5000 Impact Assessment
		Doc. No	Report NCL_CRUCIAL_D5000
		Version No	2
		Date	06.04.17



**Figure 7: Comparison of Kratie gauge data with heights from near-by altimetric points from NCL (this study) waveforms using N=40. RMS 67.8 cm (empirical retracker) and 66.9 cm (OCOg/Threshold) using  $3\sigma$  rejection level.**



		ESA Contract:	1/6287/11/I-NB
		Doc. Title	D5000 Impact Assessment
		Doc. No	Report NCL_CRUCIAL_D5000
		Version No	2
		Date	06.04.17

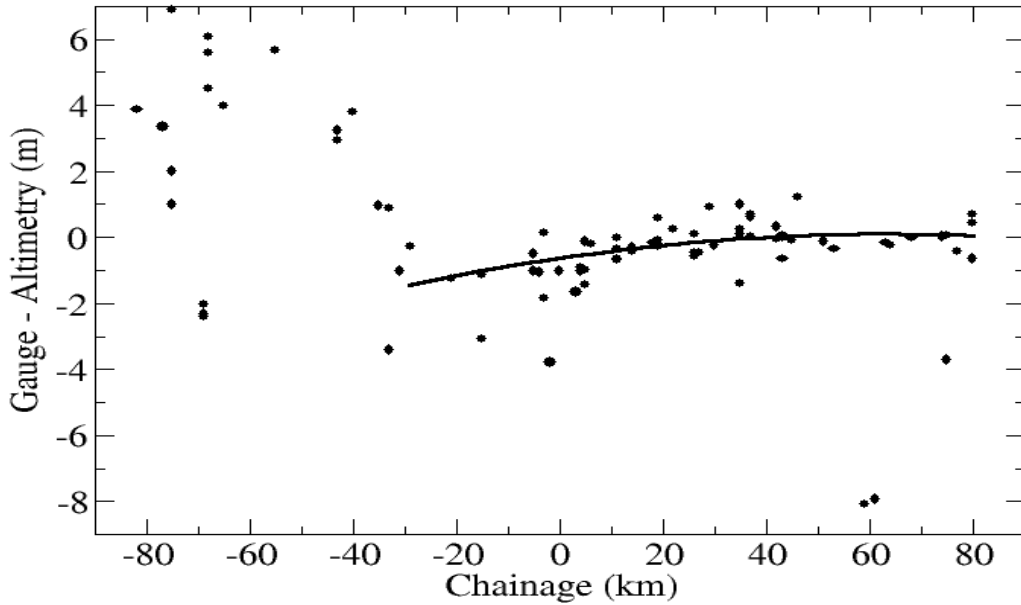




**Figure 8: Differences between gauge heights at Kratie and the CryoSat-2 heights modified for river slope (courtesy of Mekong River Commission).**

### 3.3 Amazon

FBR SAR Level 1A data available in the Amazon basin has been compared against gauges at Obidos (1.9225°S, 55.6753°W) and Manacapuru (3.3122°S, 60.6303°W) (see Figure 9 and Figure 10). At both locations, the median height over 11 points centred on the epoch nearest to the centre line was derived with heights in excess of 1 m from this value rejected. The mean and standard deviation of the measurements accepted were assumed to represent the actual values. The standard deviations typically were 5-20 cm. These RMS residuals are comparable to those across the 5 lakes in Scandanavia (Nielsen et al., 2015).

Both gauges comparisons used data over a long stretch of the river within approximately  $\pm 45$  km of the gauge. The gauge data is compared against the CryoSat-2 heights in Figure 11 and Figure 12).

At Obidos the 32 residuals between the gauge and CryoSat-2 gave an RMS value of 36.1 cm. The residuals were analysed against chainage using least squares to determine the river slope. On



		ESA Contract:	1/6287/11/I-NB
		Doc. Title	D5000 Impact Assessment
		Doc. No	Report NCL_CRUCIAL_D5000
		Version No	2
		Date	06.04.17

correcting for the slope the RMS between CryoSat-2 and the Obidos gauge data was 34.9 cm. Applying a  $2.5\sigma$  rejection criterion eliminated two data points but reduced the RMS to 27.3 cm.

Manacapuru is about 650 km upstream from Obidos. The RMS before allowing for the slope is 65.5 cm from 42 measurements. Adjusting for the slope of  $-0.429 \pm 0.024$  cm/km obtained by least squares yielded an RMS of 53.6 cm at the  $3\sigma$  rejection level.



These RMS values can be compared against published values from Topex/Poseidon (Birkett et al., 2002), In that paper, validation exercises reveal that the time series had variable accuracies with mean  $\sim 1.1$  m RMS for 1992-1999 with the best results of 0.4–0.6 m RMS from the Solimões, Amazon, Xingu and Unini rivers. Thus, the CryoSat-2 result of 53.6 cm at Manacapuru falls within the Birkett et al. (2002) best results while the CryoSat-2 result at Obidos is superior by a factor of two.

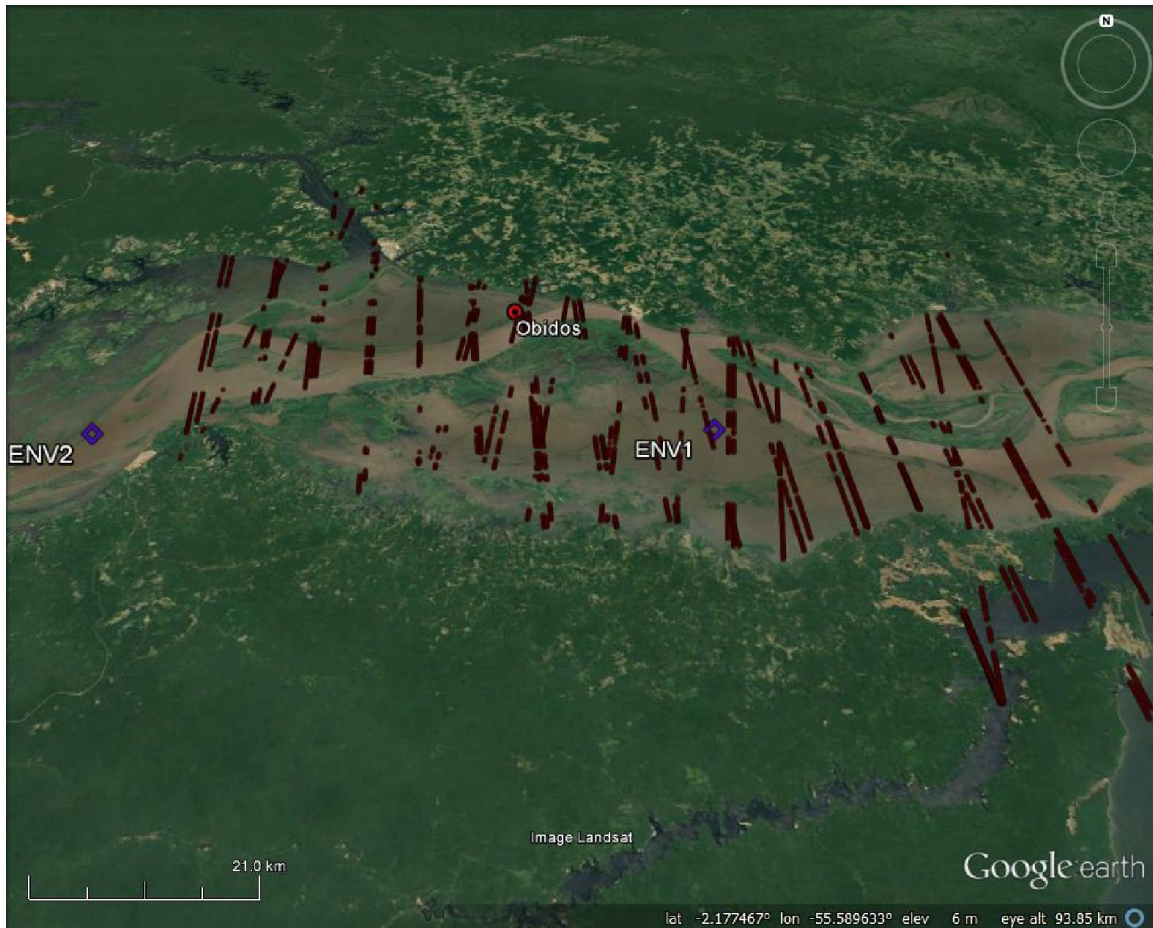
Table 6 summarises comparisons of altimetric heights available to date against data from the Obidos gauge. The comparison uses Envisat(ENV) and SARA/Altika data. The RMS from CryoSat-2 using 32 measurements is better than obtained with Envisat and nearly comparable to SARAL/Altika. The location of the crossings ENV1 and ENV2 are shown in Figure 9. ENV1 is located on Lago Grande du Curuai. The lake data will provide more measurements per pass than across the river. Given the drifting orbit CryoSat-2 data is just from the river. Note that a couple of SARAL/Altika measurements are rejected compared with none from Envisat. Again this probably reflects the susceptibility of the Ka altimeter to rain and cloud. An alternative approach for intercomparison with ENVISAT/Altika is to use CryoSat-2 passes close to the points ENV1 and ENV2. This was not attempted as the pass numbers, within say  $\pm 15$  km, would be small ( $\sim 12$ ) with an adverse effect in the statistical analyses. The approach based on estimation of the river slope is the compromise.

		ESA Contract:	1/6287/11/I-NB
		Doc. Title	D5000 Impact Assessment Report
		Doc. No	NCL_CRUCIAL_D5000
		Version No	2
		Date	06.04.17



Source	Satellite	Crossing	Date	Sigma (cm)	#
DAHITI	ENV+ALTIKA	ENV1	May 2002 - Jun2016	37.4	92(2)
	ENV		May 2002 – Oct 2010	40.2	77(0)
	ALTIKA		May 2013 – Jun 2016	17.4	15(2)
	ENV+ALTIKA	ENV2	May 2002 – Jun 2016	56.4	103(2)
	ENV		May 2002 – Oct 2010	57.7	78(0)
	ALTIKA		May 2013 – Jun 2016	26.3	25(2)
CRUCIAL	CryoSat-2	Various	Oct 2012 – Apr 2015	36.1	34(0)
	CryoSat-2		Oct 2012 – Apr 2015	34.9	34(0) slope adj
	CryoSat-2		Oct 2012 – Apr 2015	27.3	32(2) slope adj + 2.5 $\sigma$

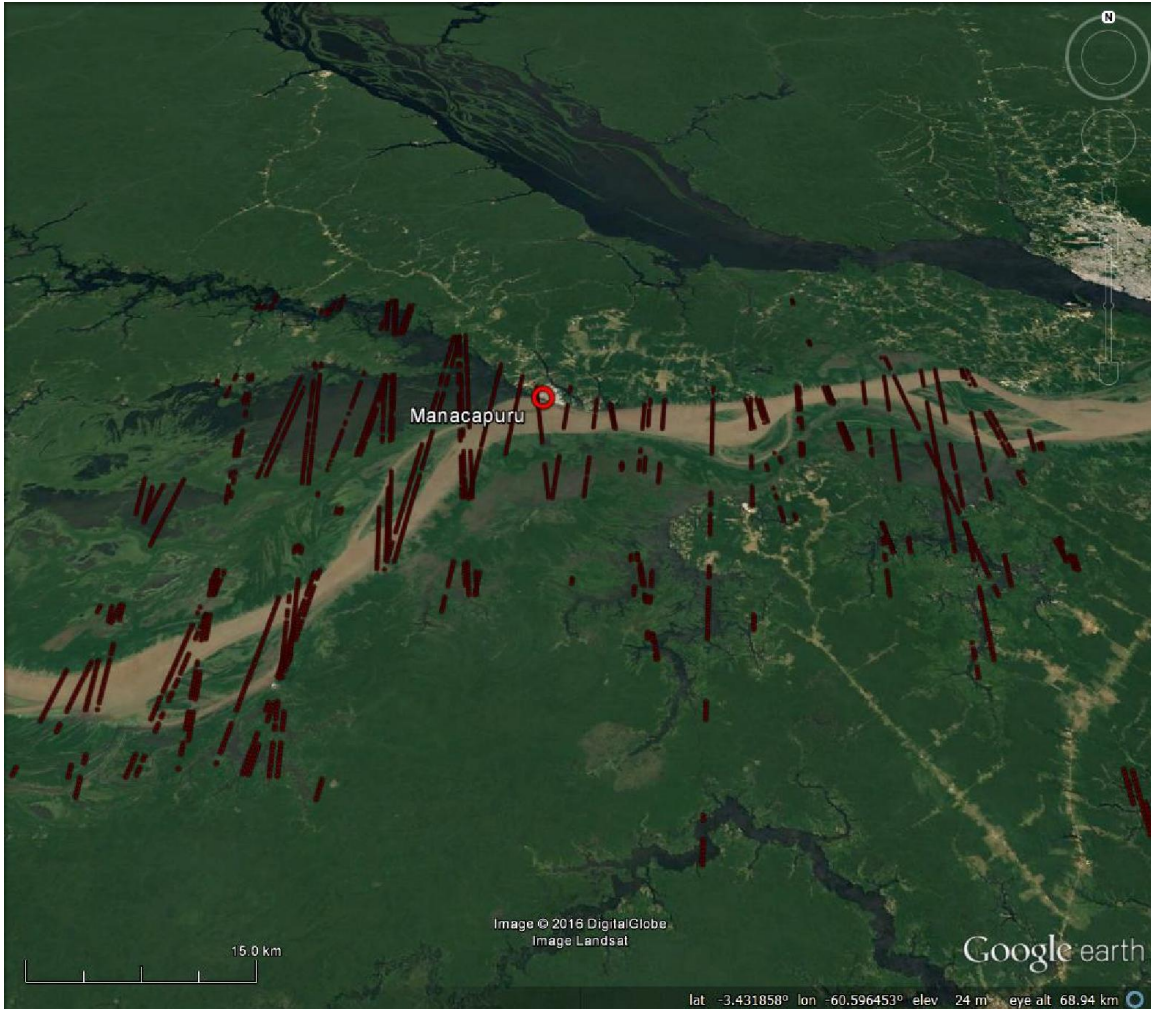
**Table 6: Comparison of altimetry against the Obidos gauge on the Amazon . Final column gives number of accepted measurements with rejected points in parenthesis.**

		ESA Contract:	1/6287/11/I-NB
		Doc. Title	D5000 Impact Assessment Report
		Doc. No	NCL_CRUCIAL_D5000
		Version No	2
		Date	06.04.17





**Figure 9: Google earth image overlaid by CryoSat-2 passes across the Amazon near the Obodos gauge (red circle) and the two ENVISAT/Altika crossing points**

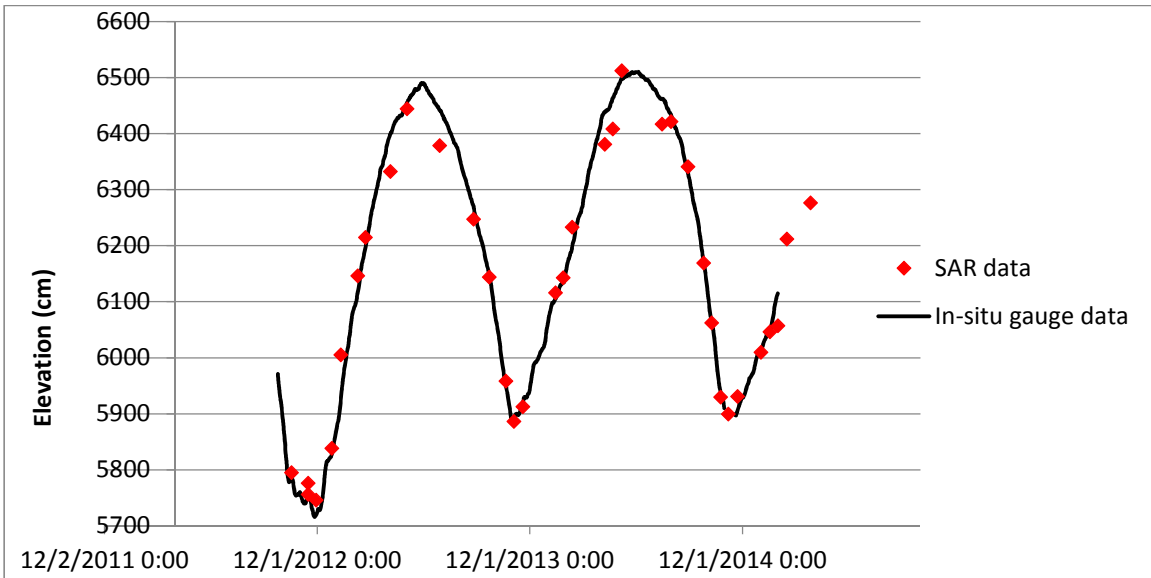
		ESA Contract:	1/6287/11/I-NB
		Doc. Title	D5000 Impact Assessment Report
		Doc. No	NCL_CRUCIAL_D5000
		Version No	2
		Date	06.04.17





**Figure 10: Google earth image overlaid by CryoSat-2 passes across the Amazon near the Manacapuru gauge (red circle) and the two ENVISAT/Altika crossing points**

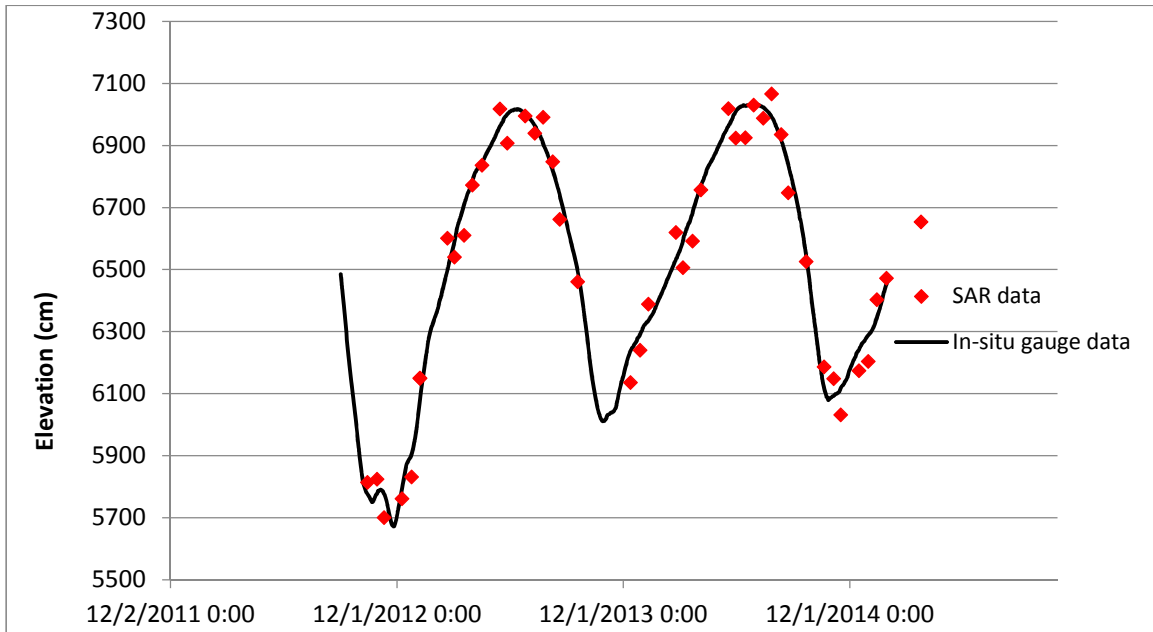


		ESA Contract:	1/6287/11/I-NB
		Doc. Title	D5000 Impact Assessment
		Doc. No	Report NCL_CRUCIAL_D5000
		Version No	2
		Date	06.04.17





**Figure 11: FBR SAR heights (N=40, empirical retracker) at Obidos using both a  $2.5\sigma$  rejection level and slope adjustment (RMS 27.3 cm).**

		ESA Contract:	1/6287/11/I-NB
		Doc. Title	D5000 Impact Assessment
		Doc. No	Report NCL_CRUCIAL_D5000
		Version No	2
		Date	06.04.17



**Figure 12: FBR SAR heights (N=40, empirical retracker) at Manacapuru using both a 3 $\sigma$  rejection level and slope adjustment (RMS 53.6 cm).**

		ESA Contract:	1/6287/11/I-NB
		Doc. Title	D5000 Impact Assessment
		Doc. No	Report NCL_CRUCIAL_D5000
		Version No	2
		Date	06.04.17

## 4 SARin FBR Product and Validation

The analysis of the waveforms from the two antennae in SARin mode assumes that the two waveforms illuminate the same surface area. If the satellite roll is accounted for, heights from the two antennae should be near identical over flat terrain and inland waters. Disparity between the measurements can then be used as a quality control with any difference identifying inconsistencies. Use can also be made of the phase difference between the waveforms and the coherence from the two antennae to investigate the cross angle.

### 4.1 Amazon

#### 4.1.1 SARin Heights



As an exemplar of SARin over inland water, we consider passes across the Amazonas near the Tabatinga gauge. Analysis in D4200 showed little discernible height difference between the right and left antennae and between OCOG and the use of empirical retracker. Also, commented in D4200 is the value of  $N = 60$  for SARin (all waveforms in multi-look used) compared with  $N = 40$  for SAR case.

In contrast the G-POD SARvatore heights reveal a larger variance. As for the SAR data, the cause of the discrepancy is the use of the SAMOSA2 retracker rather than the waveforms which have already been proved to be similar.

#### 4.1.2 Validation against gauge data at Tabatinga calibration

The Amazon near Tabatinga is plotted as Figure 13 for a stretch of the river some 150 km in length. Only data across the Amazon itself has been used although data was available from the tributary (Rio Javari) in the lower left quadrant of Figure 13. The stretch used has SARin mode passes that are about 2 days apart, but differ in longitude by  $1.2^\circ$ . Thus, given the small time difference we can assume that the derived SARin mode heights record the same river flows. The difference between the SARin river heights at the two locations provides an estimate of the slope of the





		ESA Contract:	1/6287/11/I-NB
		Doc. Title	D5000 Impact Assessment
		Doc. No	Report NCL_CRUCIAL_D5000
		Version No	2
		Date	06.04.17

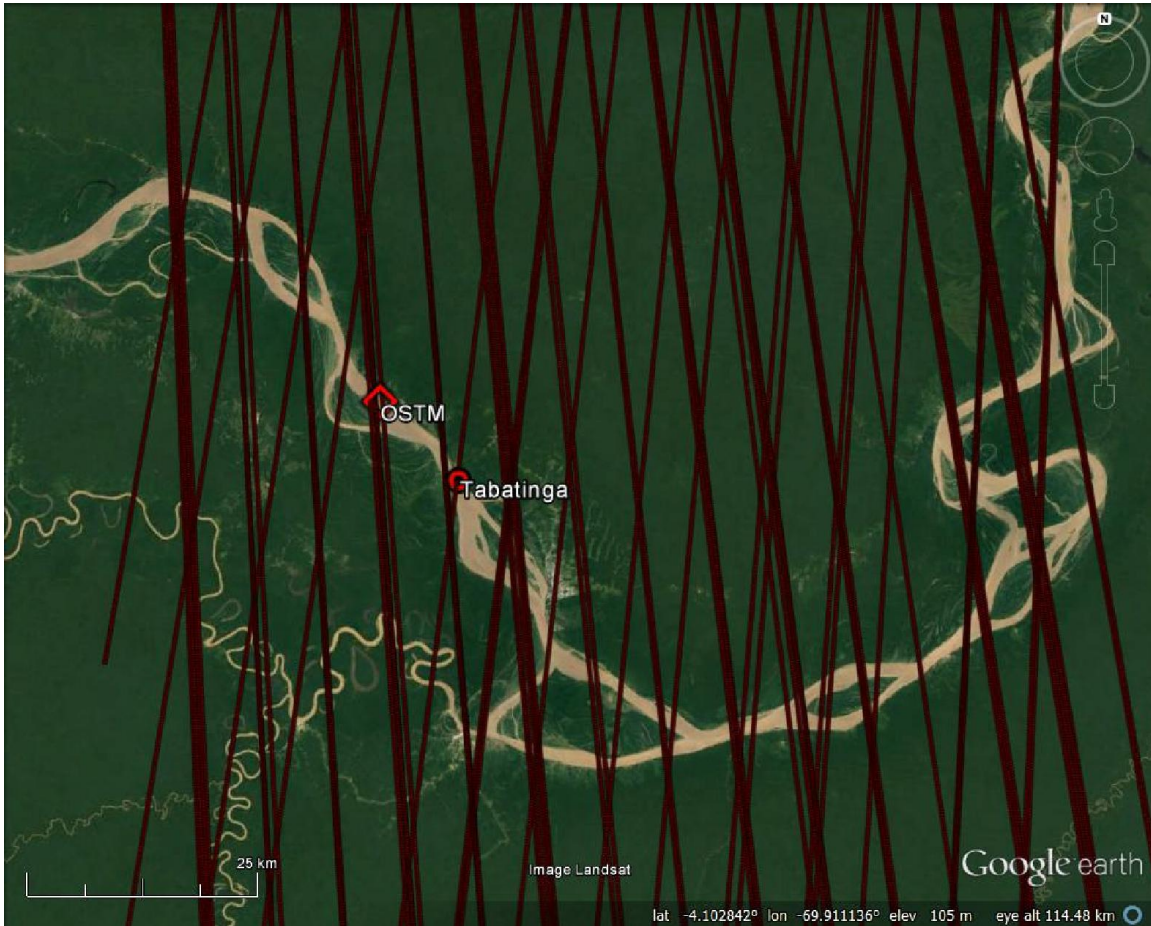
river. Taking the average of these values gives a river slope of -4.42 cm per km along the river. This is equivalent to a ground slope of  $-0.0025^\circ$ . On using this altimeter derived river slope and the location of the 64 crossings of the Amazon near Tabatinga, a slope corrected set of heights was obtained. The corrected heights, using RMS distances based on the centre line and the gauge data are plotted as Figure 14. The agreement between gauge and altimetry has RMS of 29.9 cm on eliminating two outliers. This fit is significantly better than that seen at Manacapuru although some 1500 km further upstream and similar to that at Obidos. The CryoSat-2 value is also comparable to the RMS of 29.1 cm from 445 points of a Jason-2/OSTM crossing (see Figure 13) of the Amazon about 8 km from the gauge.

Similar to the comments for passes acquired near Obidos, the preferred approach utilized passes over a long river stretch with correction applied for river slope. The alternative approach of restricting CryoSat-2 passes close to the gauge (or Jason-2/OSTM crossing) would again lead to questionable statistics.



Conclusion: Despite utilizing crossings over a 150km stretch the CryoSat-2 agreement with the Tabatinga gauge data is comparable to the Jason-2/OSTM DAHITI gauge data for a crossing just 8 km from the gauge.

The SARin data has been used to derive the cross angle. The interpretation of the cross angle as the ground slope is, however, mostly incorrect as discussed previously. The cross angle for 64 passes near Tabatinga are plotted as Figure 15 and summarized in Table 7. This figure shows a negative cross angle for both the North-South and South-North passes across the Amazon near the Tabatinga gauge. For confidence in the solution, the river slope should change sign with the pass direction. However, the roll-bias is subject to some uncertainty. If we allow the slope to change sign with the pass direction and then solve for a further roll-bias we infer a roll-bias correction of  $-0.004^\circ$  and a slope of  $-0.0032^\circ$ . This is close to the expected value but the 95% confidence interval is twice this value.

		ESA Contract:	1/6287/11/I-NB
		Doc. Title	D5000 Impact Assessment Report
		Doc. No	NCL_CRUCIAL_D5000
		Version No	2
		Date	06.04.17



**Figure 13: Google earth image of Amazon near Tabatinga; gauge marked as red circle with Jason-2/OSTM crossing denoted by red diamond.**

		ESA Contract:	1/6287/11/I-NB
		Doc. Title	D5000 Impact Assessment
		Doc. No	Report NCL_CRUCIAL_D5000
		Version No	2
		Date	06.04.17

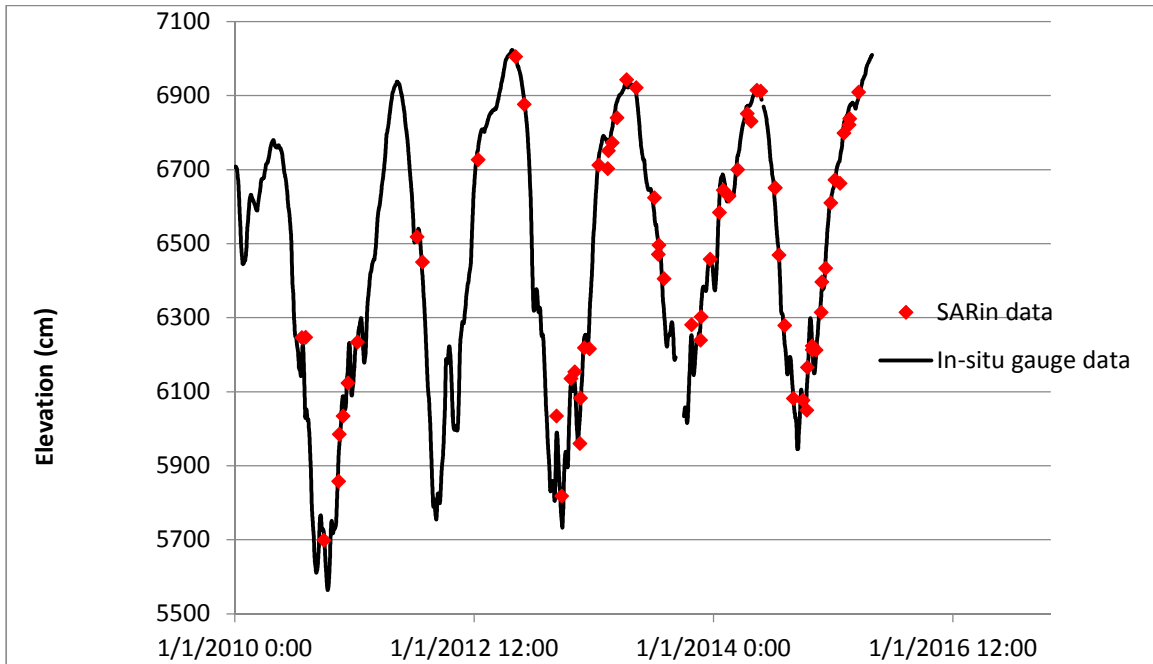


Figure 14: Tabatinga gauge heights and CryoSat-2 SARin (N=60, OCOG/Threshold) heights corrected for river slope. RMS difference 29.9 cm.

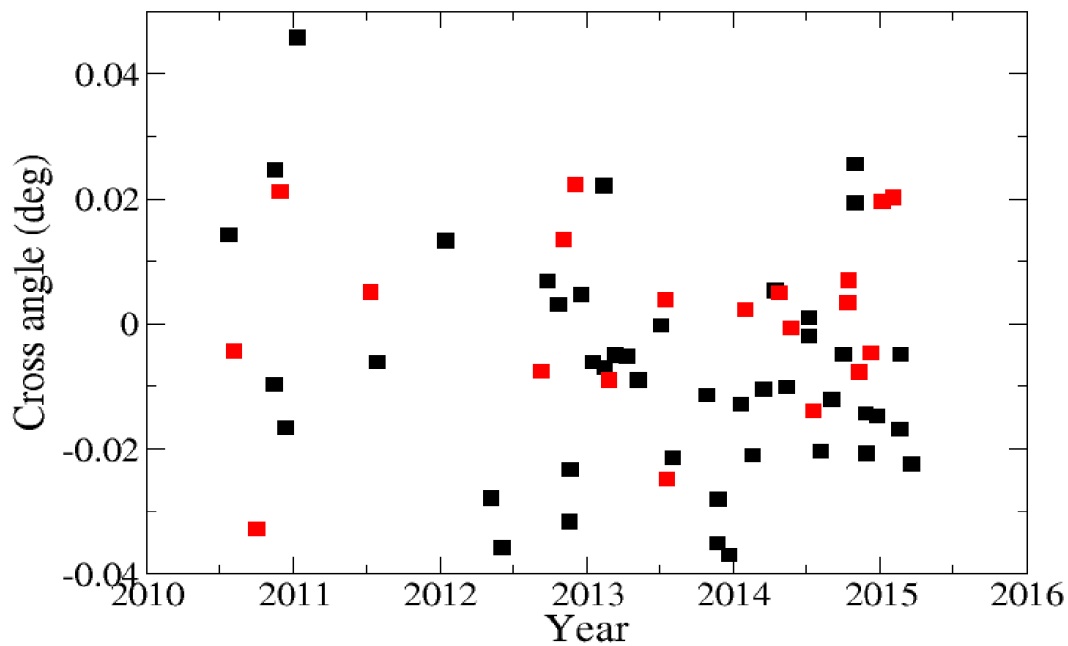




Figure 15: Plot of the 64 accepted cross angles comprising 44 ascending passes (black squares) and 20 descending passes (red squares).

		ESA Contract:	1/6287/11/I-NB
		Doc. Title	D5000 Impact Assessment
		Doc. No	Report NCL_CRUCIAL_D5000
		Version No	2
		Date	06.04.17

Pass	#	Mean (deg)	95% confidence (deg)
All	64	-0.0053	0.0054
Ascending	44	-0.0072	0.0053
Descending	20	-0.0009	0.0065

**Table 7: Statistics of cross track angles from the 64 passes near Tabatinga. The expected value of the slope from SARin height differences is -0.0025°.**



#### 4.1.3 Analysis of the cross angle near the Tabatinga gauge

Figure 16 shows waveforms from the two antennae, the coherence and the phase for two locations over the Amazon. The left hand location (#274) is -3.929538°S, 70.207448°W with the adjacent (#275) at 3.926810°S, 70.207730°W in the right-hand column. The waveforms from the left and right antennae are near identical at both locations while the maximum coherence near the retrack point is 0.86 and 0.85 respectively for #274 and #275. The least squares estimated cross angle is 0.0296° for location #274 and 0.036° for location #275.

The differences between the heights from the two antennae and the cross angle as derived from the waveform bin phases are plotted as Figure 17. The Amazonas flood plain is visible as the latitudinal extent of low variability centered on 4.2°S. The difference in height measurements between the two antennae has a mean near zero and standard deviation near 1 cm. Note, differently from section 2.4, this difference uses the convention of height from the right antennae minus height from the second (left-side) antenna with antennae as orientated along the flight direction.

Conclusion: The two antennae provide height measurements to within 1 cm (standard deviation) over flat areas.



The interpretation of the cross angle is illustrated in Figure 18 where the upper plot shows the ground point locations of the 5 May 2012 ascending pass close to the Amazon while the lower plot aligns the cross angle. A positive offset of 0.025° was added to the cross angle to give a mean

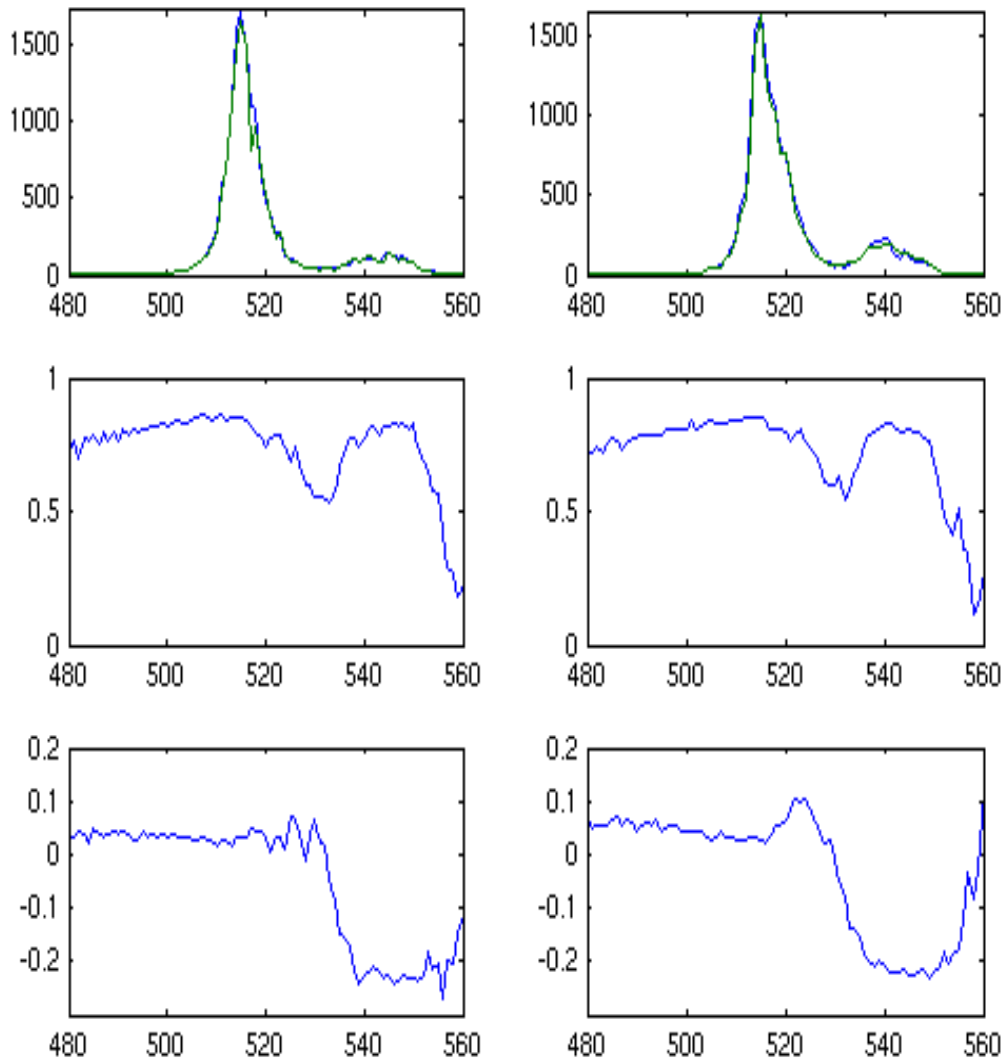
		ESA Contract:	1/6287/11/I-NB
		Doc. Title	D5000 Impact Assessment
		Doc. No	Report NCL_CRUCIAL_D5000
		Version No	2
		Date	06.04.17

value near zero when the satellite was over the Amazon. A positive cross angle means that the dominant water body forming the leading edge of the waveform is under the right hand antenna and conversely for a negative cross angle. Thus the large and negative cross angle near latitude 3.83°S is a response to the Amazon being to the left of the flight direct direction. The positive cross angles at the start of the pass are representative of a dominant reflectance from the right of the flight direction. Some care must be exercised as the actual extent of the Amazon at this time may differ from the Google earth image. Note that once the water body is outside the cross-track footprint the above interpretation of the cross-angle will no longer hold. The cross-angle will now be dominated by non-water reflectance with the expectation that the cross-angle will represent land reflectance. As seen in Figure 18, the footprint is over land in the first instance before the river enters the footprint. Similarly, towards the end of the pass the river will leave the footprint but now the small tributary contributes giving both a smaller variation than at the start of the pass and a cross-angle that is slightly positive as expected from reflectance to the right of the flight direction.



Other passes have been examined with results presented in D4200.

Conclusion: In general the cross track angle is relatively noisy due to the complex nature of saturated ground and inland water. However, the plots generally show the expected behaviour of the cross angle particularly for large excursions of the river to left or right of the flight path.

		ESA Contract:	1/6287/11/I-NB
		Doc. Title	D5000 Impact Assessment Report
		Doc. No	NCL_CRUCIAL_D5000
		Version No	2
		Date	06.04.17



**Figure 16: SARin waveforms (upper), coherence (middle) and cross angle in degrees (lower). In the upper plot the right antennae is coloured blue and the left antennae is green. X-axis is bin number; Y axis is power (upper), coherence (middle) and degree (lower). Left hand column location #274 (3.930 °S 70.207 °W); right hand column location #275 (3.927 °S 70.207 °W). Date of pass 5 May 2012.**

		ESA Contract:	1/6287/11/I-NB
		Doc. Title	D5000 Impact Assessment
		Doc. No	Report NCL_CRUCIAL_D5000
		Version No	2
		Date	06.04.17

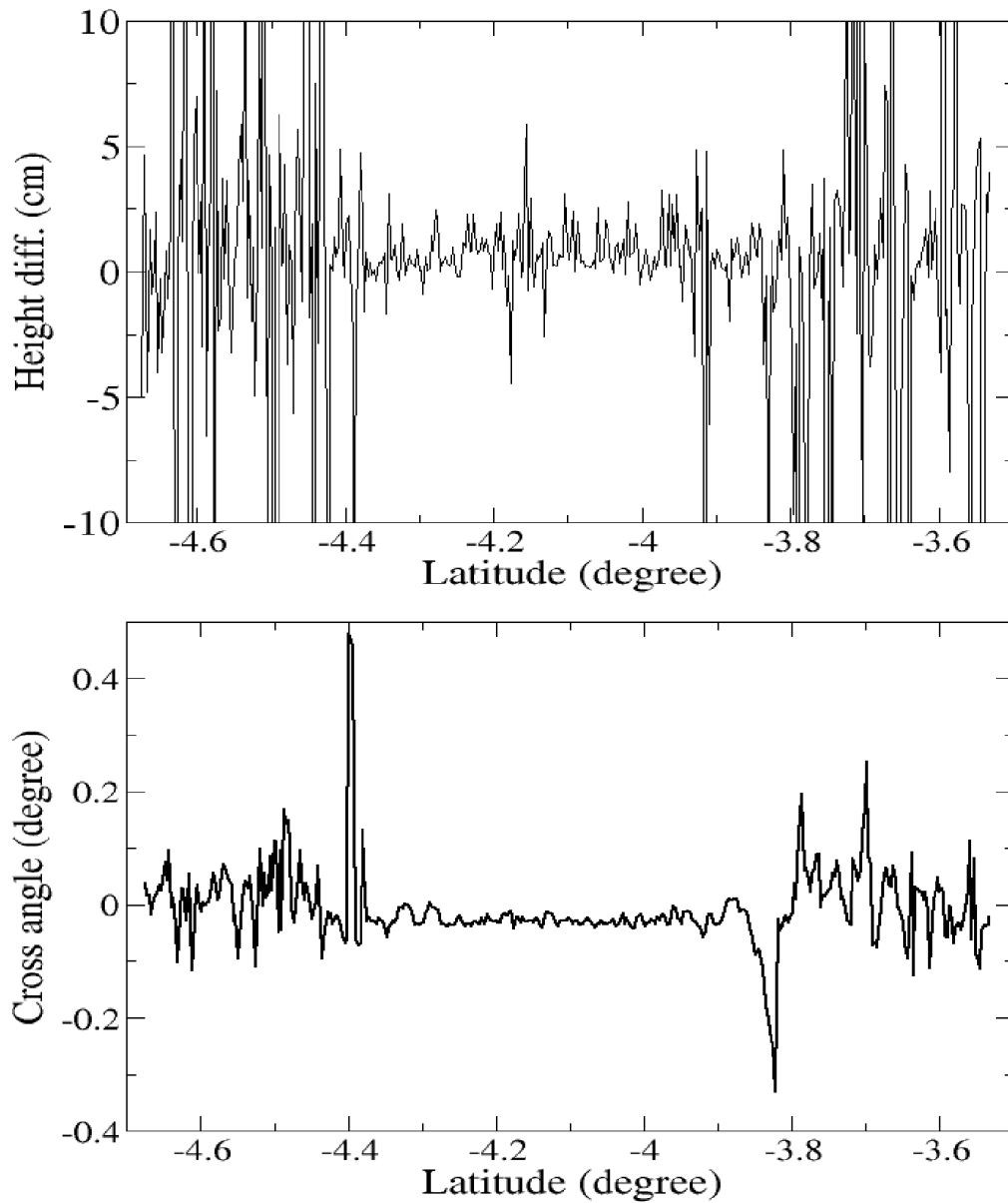




Figure 17: OCOG/Threshold based difference between heights from the two SARin antennae (Upper). Cross angle (Lower). SARin Amazonas 5 May 2012. (Latitude -4.2° corresponds to longitude 70.179°W).



		ESA Contract:	1/6287/11/I-NB
		Doc. Title	D5000 Impact Assessment Report
		Doc. No	NCL_CRUCIAL_D5000
		Version No	2
		Date	06.04.17

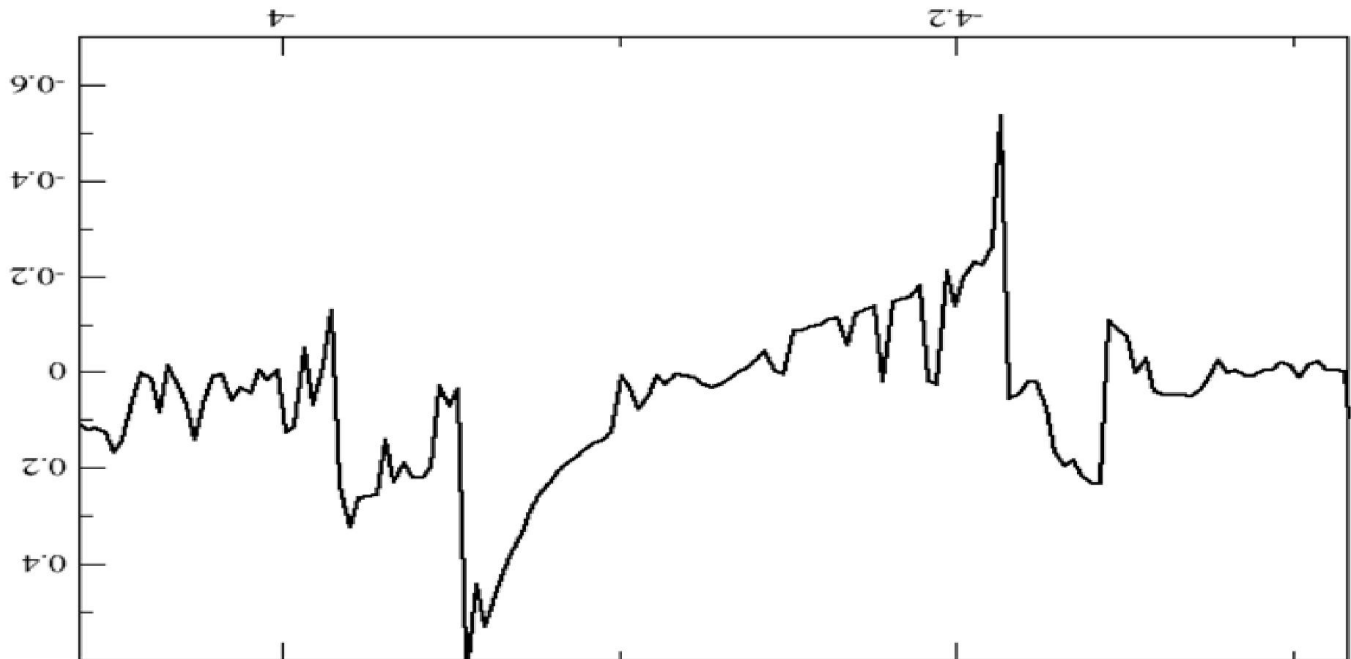




Figure 18: Google earth plot of descending pass on 8 September 2012 across Amazon near Tabatinga (upper). Cross angles from SARin mode (lower). The blue arrow points along direction of flight.





		ESA Contract:	1/6287/11/I-NB
		Doc. Title	D5000 Impact Assessment
		Doc. No	Report NCL_CRUCIAL_D5000
		Version No	2
		Date	06.04.17

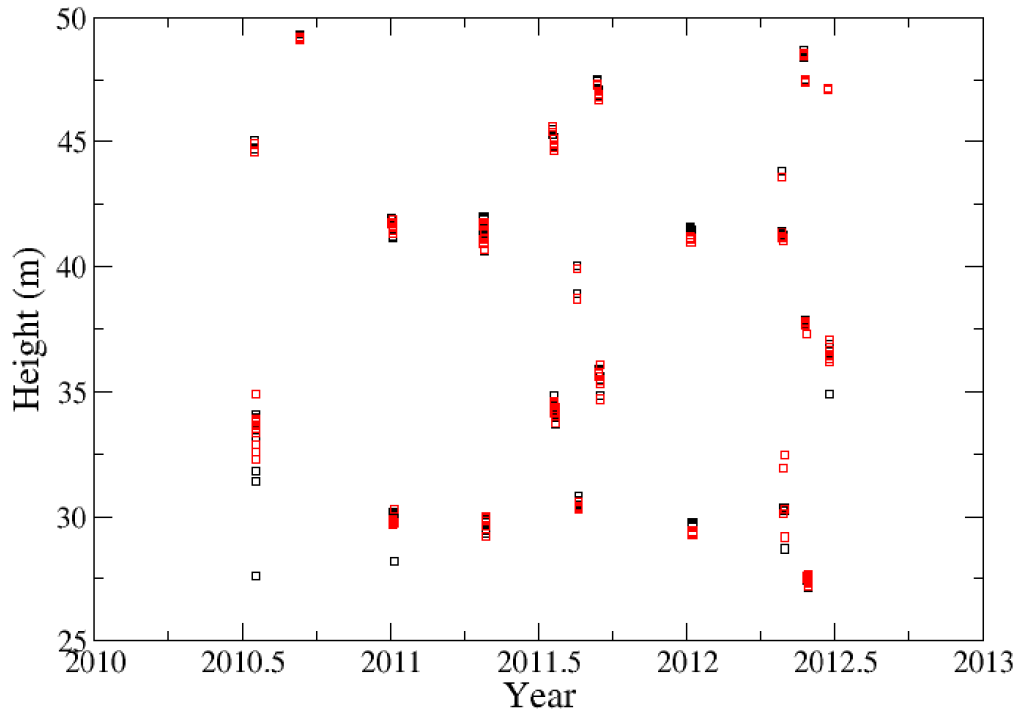
## 4.2 Brahmaputra

The Mekong and Amazon were the primary target for L1A waveform analysis. However, CRUCIAL included a hydrological modelling component (see section 6) over the Brahmaputra. Given the complexity of the waveform analysis results for the Brahmaputra were not available until late into the study. To avoid unnecessary delay DTU utilized heights derived by other researchers at DTU from retracked L1B waveforms.



The values from the two solutions and the difference between the NCL and DTU values are plotted as Figure 19 and Figure 20 respectively. Some outliers are evident. Points were rejected based on the median value and extending the window of data accepted to include all points within  $3\sigma$  of the window mean. In practice hydrological assimilation requires a single value from the river crossing and use of say the median value would mitigate against spurious values. These two figures involve data from 35 passes across the Brahmaputra some of which are a few days apart and thus the passes are indistinguishable on the time series plot. 170 heights out of the possible 185 heights were accepted. The mean difference was 11.8cm with standard derivation of 15.7 cm. The 12 cm offset is due to different procedures including the threshold for retracking. More important is the scatter in the data and with a standard deviation of just 16 cm which is a factor of 2 lower than the scatter in the data seen through comparisons with in situ gauge data.

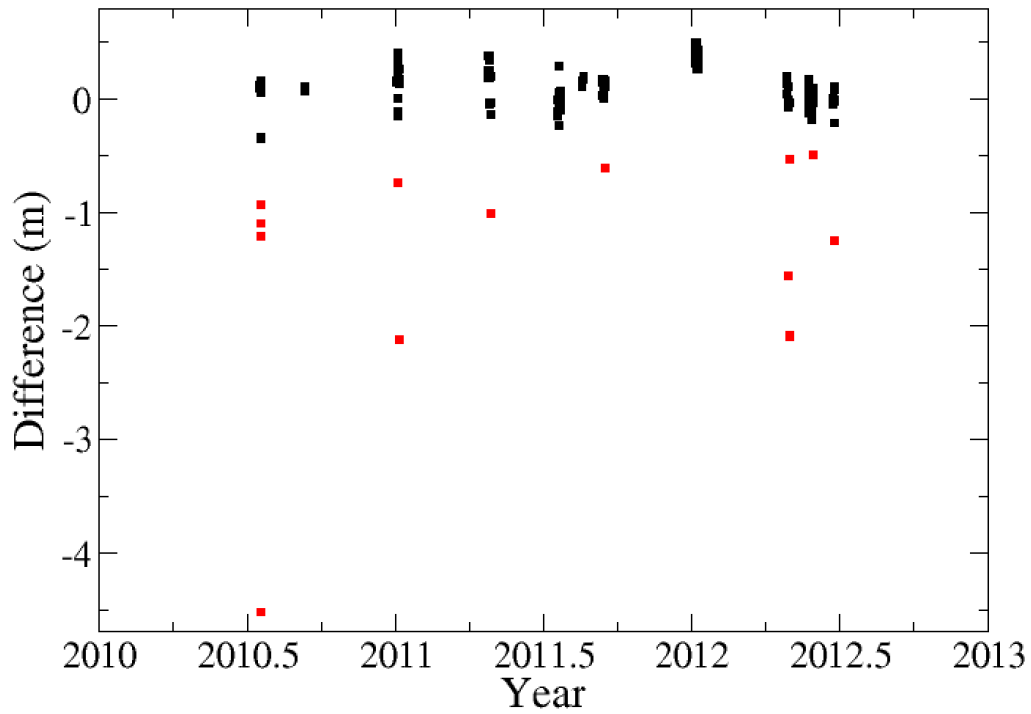
Conclusion: The difference between CRUCIAL heights over the Brahmaputra and those derived by DTU from 20 Hz L1B retracked waveforms is a factor two lower that the scatter seen in comparisons against in situ gauge data. Thus, we are confident that the data set used in the hydrological assimilation and modelling is of high accuracy.

		ESA Contract:	1/6287/11/I-NB
		Doc. Title	D5000 Impact Assessment Report
		Doc. No	NCL_CRUCIAL_D5000
		Version No	2
		Date	06.04.17





**Figure 19: CryoSat-2 SARin heights across the Brahmaputra. CRUCIAL heights (N=60, OCOG/Threshold) (black squares) and DTU derived heights (red squares).**

		ESA Contract:	1/6287/11/I-NB
		Doc. Title	D5000 Impact Assessment
		Doc. No	Report NCL_CRUCIAL_D5000
		Version No	2
		Date	06.04.17





**Figure 20: The height difference between NCL and DTU heights across the Brahmaputra. Accepted points denoted by black squares, rejected points by red squares. Mean difference and standard deviation of accepted points 11.9cm and 15.8 cm, respectively.**

		ESA Contract:	1/6287/11/I-NB
		Doc. Title	D5000 Impact Assessment
		Doc. No	Report NCL_CRUCIAL_D5000
		Version No	2
		Date	06.04.17



## 5 Summary of validation of FBR SAR and SARin inland water heights

The above sections detail the validation of heights derived by processing SAR and SARin FBR L1A data. This section, taken from D4200, details the significant conclusions drawn from the CRUCIAL waveform analyses for inland water studies.



- The speckle in the burst echoes affects the recovered heights from the 80 Hz SAR data and multi-look waveforms are essential for precise heights.
- The number of stacked waveforms used in the construction of the multi-look waveform is important for SAR altimetry. A reduction from the maximum possible number in the stack of approximately 240 (N=120) to say 81 (N=40) waveforms centred on the beam directed closest to nadir has been seen to reduce the variability in derived heights across Tonlé Sap.
- The reduction from N=120 to N=40 in the waveform stack sharpens the leading edge of the multi-look waveform. The change in N causes an offset between the derived heights which is indistinguishable from other contributions to the altimeter bias. In consequence, a fixed value for N must be applied to all analyses to avoid bias.
- The G-POD SARvatore and SARinvatore waveforms are almost identical to those derived within CRUCIAL on using N=120 or N=123.
- The use of a Hamming window (cosine weighting) is recommended (see Table 1).
- The difference between the empirical retracers and OCOG/Threshold is not significant. More advanced retracers or the use of auto-correlation between consecutive waveforms across large lakes might change this conclusion. Variability in height recovery has been shown to be 5 cm across Tonlé Sap for multi-look SAR data at about 20 Hz. This is equivalent to a precision of 1-2 cm in 1 Hz data.
- Validation of altimetric heights across Tonlé Sap is affected by distance from the gauge. For OSTM a 12 day lag has been inferred with respect to the Prek Kdam gauge. This lag increases with distance of the pass from Prek Kdam as shown by the auto-correlation analysis between the Prek Kdam and Kumong Luong gauges. The agreement between Prek Kdam and OSTM of 42.6 cm is slightly reduced to 42.1 cm between Prek Kdam and CryoSat-2. The latter assumes the time lag for all CryoSat-2 non-repeating passes is that of OSTM (i.e. 12 days) and that the EGM08 geoid is accurate. Since the former, in particular, has been shown to be incorrect there is evidence that CryoSat-2 is performing better than OSTM across Tonlé Sap.

		ESA Contract:	1/6287/11/I-NB
		Doc. Title	D5000 Impact Assessment
		Doc. No	Report NCL_CRUCIAL_D5000
		Version No	2
		Date	06.04.17

- The SAMOSA2 retracking in G-POD is inappropriate for inland waters as seen by the statistics across Tonlé Sap in Table 1. Retracking the G-POD waveforms using the empirical trackers developed in CRUCIAL or with the OCOG/Threshold retracker yields enhanced results.
- Validation of CryoSat-2 inland water heights along the Mekong are severely affected by the non-repeating orbit. Correction based on low flow river slope is not exact as the gauges show a difference in range and hence a change in slope at high flow.
- A comparison of the OCOG/Threshold (RMS 66.9 cm) and empirical retrackers (67.8 cm) for N=40 shows a slight preference for the OCOG/Threshold retracker. These differences are comparable to those of Birkinshaw et al (2010) where an RMS of 76 cm was seen for ERS-2 for the years 1995-2003 and 57 cm for Envisat for the years 2002-2008.
- FBR SAR data close to the Obidos gauge on the Amazon allowed the river slope to be computed from the gauge/altimetry residuals and chainage. Using least squares to determine the river slope. The recovered slope was -0.22 cm per km. On correcting for the slope the RMS between CryoSat-2 and the Obidos gauge data was 34.9 cm and applying a  $2.5\sigma$  rejection criterion eliminated two points but reduced the RMS to 27.3 cm. The slope with  $R^2 = 0.07$  was just positive. At Manacapuru, 650 km upstream from Obidos, the RMS, after similarly allowing for the slope, was 53.6 cm. Here the slope of  $-0.429 \pm 0.024$  was well determined with  $R^2 = 0.89$ . These RMS values can be compared against Birkett et al. (2002), where best results from Topex/Poseidon for 1992-1999 were in the range 0.4–0.6 m RMS. Thus, the Manacapuru RMS falls within the Birkett et al. (2002) best results while the CryoSat-2 result at Obidos is superior by a factor of two.
- Over the inland waters utilised in this study CryoSat-2 is comparable or slightly more accurate than ENVISAT and Jason-2/OSTM but probably less accurate than SARAL/Altika. Although only a small number of SARAL/Altika measurements are available to date a few epochs are classified as outliers. This may reflect the susceptibility of the Ka altimeter to cloud and rain.
- Heights from SARin FBR data in the vicinity of the gauge at Tabatinga yielded an RMS of 29.9 cm. Again this is an improvement on the best results of Birkett et al. (2002) for the Amazon.
- The SARin cross angle is dominated by the location of the dominant water surface reflectors in the cross-track footprint slice. This inference will be extended in future projects/studies to investigate the utility of the SARin derived cross angle to correct the off-nadir altimetric height.
- In general the cross track angle recovered from SARin FBR data is relatively noisy due to the complex nature of saturated ground and inland water. However, the results generally show the expected behaviour of the cross angle particularly for large excursions of the river to left or right of the flight path.

		ESA Contract:	1/6287/11/I-NB
		Doc. Title	D5000 Impact Assessment
		Doc. No	Report NCL_CRUCIAL_D5000
		Version No	2
		Date	06.04.17

- Heights for the Lower Brahmaputra derived by DTU from SARin L1B waveforms retracked using a primary peak threshold retracker were consistent with results obtained within CRUCIAL from L1A data. A 12 cm offset is due to the different procedures including the waveform construction and threshold for retracking. More important is the scatter in the data and with a standard deviation of just 16 cm. We are thus confident that the DTU data used in the Data Assimilation work is of high accuracy.

		ESA Contract:	1/6287/11/I-NB
		Doc. Title	D5000 Impact Assessment
		Doc. No	Report NCL_CRUCIAL_D5000
		Version No	2
		Date	06.04.17



## 6 Informing regional-scale hydrodynamic models with CryoSat-2 Altimetry

(By Peter Bauer-Gottwein and Raphael Schneider)

The ESA CRUCIAL project has been one of the first attempts to systematically explore the value of CryoSat-2 altimetry data for river analysis and modeling. The project has generated new knowledge and insight that can support future applications of the mission over rivers. Main findings fall into the following areas:

- From a hydrologist's perspective, the main difference between CryoSat-2 and previous altimetry missions is the orbit configuration with its 369-day exact repeat and 30-day sub-cycle. This orbit configuration results in a dense and irregular sampling pattern over rivers, which is different from the classical virtual station time series derived from other altimetry missions.
- Before CryoSat-2 data can be used for river analysis and modeling, they have to be pre-processed. For virtual station data, outlier removal in the time series dataset has been fairly straightforward, because consistency of the time series can be checked and used to identify outliers (e.g. Nielsen et al., 2015). This option is not available for CryoSat-2 altimetry over rivers. Accurate water masks are therefore required to identify whether or not an individual recorded echo originates from the river water surface. Moreover, uncertainty assessment of derived heights remains a challenge but can be partly addressed by aggregating individual returns into spatial clusters.
- One unique characteristic of the CryoSat-2 altimetry dataset is its very dense spatial resolution with a ground-track separation of just 8 km at the equator (Wingham et al., 2006). The dataset thus provides a complete and dense mapping of the river water level profile as compared to virtual station datasets that are many tens of kilometers apart for Envisat/Sentinel-3. This information can be used to estimate river morphology parameters such as river bed elevation and flow-cross-sectional shape at high spatial resolution (Schneider et al., 2016b).
- CryoSat-2 data can be assimilated to hydrodynamic models to obtain, at each point in time, the best estimate of river water level based on both model predictions and satellite observations. In order to assess the value of CryoSat-2 data in this context and compare it to



		ESA Contract:	1/6287/11/I-NB
		Doc. Title	D5000 Impact Assessment
		Doc. No	Report NCL_CRUCIAL_D5000
		Version No	2
		Date	06.04.17

that of other missions, synthetic data assimilation experiments are instructive. In such experiments, perfect statistical consistency between the model and the observational dataset is ensured as synthetic observations are produced from simulated model outputs (Schneider et al., 2016a).



- Finally, real CryoSat-2 observations can be assimilated to hydrodynamic models and the impact of the data assimilation on sharpness and reliability of predictions can be assessed. Performance can also be compared to synthetic data assimilation experiments, which yields useful insight into future directions for model development and altimetry data processing (Schneider et al., 2016a).

Our main findings within these five domains are briefly summarized and illustrated here with a focus on their potential impact on future research and application of satellite radar altimetry over inland waters and especially rivers.

## 6.1 Implications of the orbit configuration for hydrologic analysis

CryoSat-2 is on an exact repeat orbit of 369 days duration with a 30 day subcycle. Within each subcycle, the satellite returns to the same region of the planet at daily intervals. However every day, the nadir point of the satellite moves by several tens of kilometers to the west (“drifting orbit”). The orientation of the river with respect to the orbit ground track therefore determines the spatio-temporal sampling pattern of CryoSat-2 for any river.

- If the river flows from east to west (e.g. Brahmaputra, Congo), the orbit drift direction is aligned with the flow direction. However, for most rivers, the orbit drift speed is lower than the wave velocity in the river. Therefore, CryoSat-2 samples will “fall behind” a wave front traveling down the river.
- If the river flows from west to east (e.g. Amazon, Yangtze), orbit drift direction and flow direction are opposite. At some point in time, there will be a cross-over between a flood wave coming down the river and the orbit drift.
- For both east-west and west-east flowing rivers, any subcycle will include periods with daily samples of river level and periods of no data. This is because at some point during the subcycle, the orbit will drift into the longitude range covered by the river and at some point it will drift out of it again. For the Assam Valley stretch of the Brahmaputra (east-west extent about 600 km), a subcycle would typically include 10 days with daily data followed by 20 days without data.
- For north-south or south-north oriented rivers, there will be a very short period in which data is available at very high spatial resolution followed by long periods without any data.

		ESA Contract:	1/6287/11/I-NB
		Doc. Title	D5000 Impact Assessment
		Doc. No	Report NCL_CRUCIAL_D5000
		Version No	2
		Date	06.04.17

However, the river might be observed at several, distant locations for the same overflight of CryoSat-2.

To illustrate the CryoSat-2 spatio-temporal sampling pattern for rivers, Figure 21 shows the situation for the Assam Valley in the Brahmaputra system.

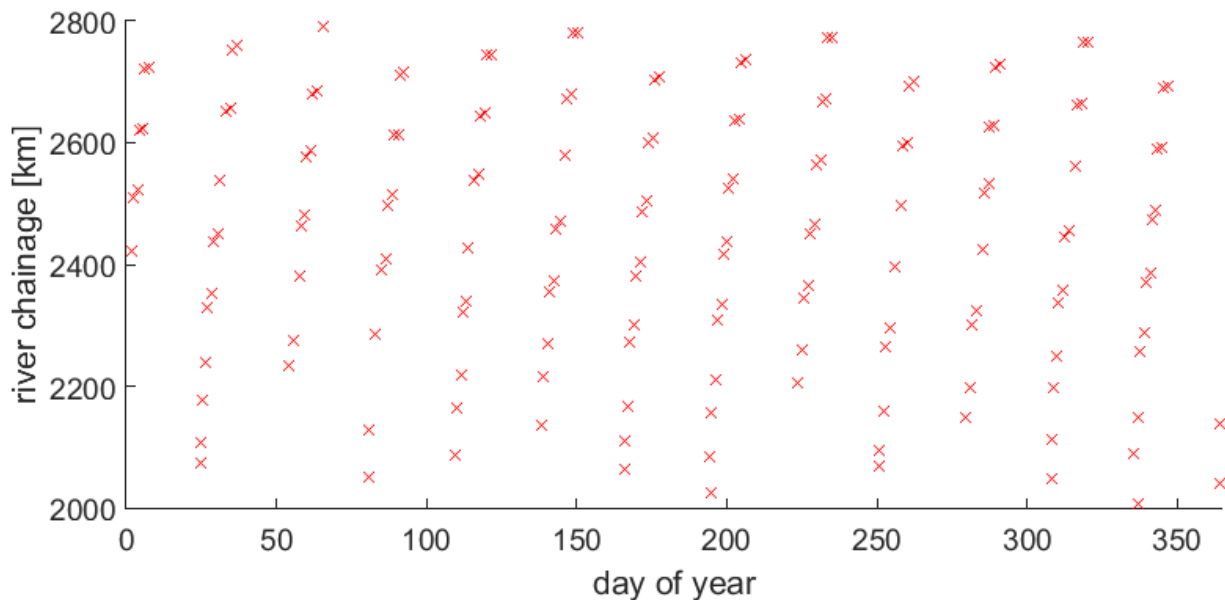




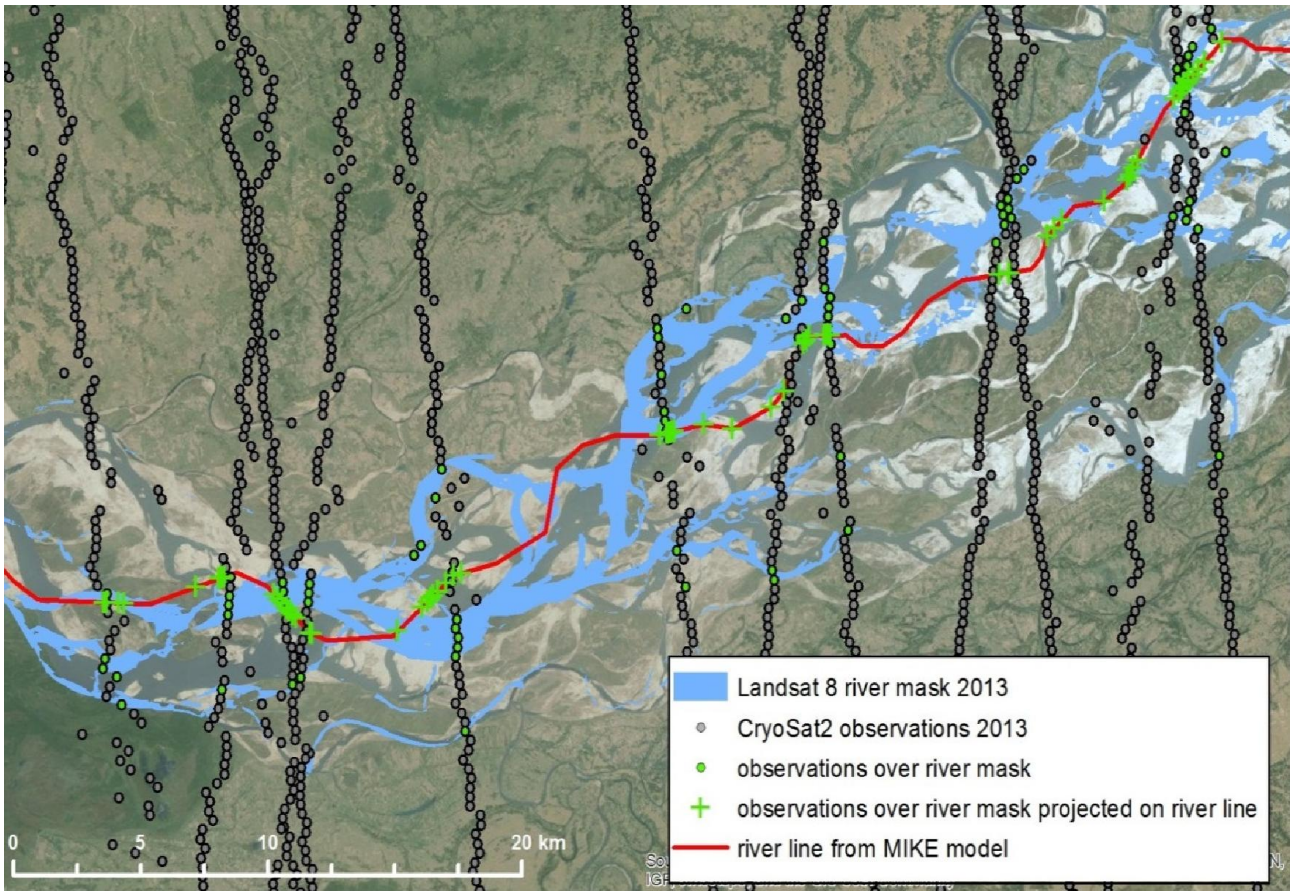
**Figure 21: CryoSat-2 sampling pattern over the Brahmaputra in the Assam Valley for the year 2012**

## 6.2 Preprocessing of CryoSat-2 altimetry

In order to identify water returns in the CryoSat-2 dataset, high-resolution, temporally resolved open water masks are required. It is impossible to reliably determine from the CryoSat-2 data alone, if the return comes from water or land surfaces. There are basically two ways to generate open water masks at regional scale: Multi-spectral and thermal data, e.g. from Landsat (Figure 22, Carroll et al., 2009; Schneider et al., 2016b) or SAR imagery, e.g. from Sentinel-1 (Westerhoff et al., 2013). SAR imagery has the advantage of being unaffected by cloud cover, while optical and thermal data can only be used under cloud-free conditions.



Many rivers display significant variations in river width and channel location and ideally, multi-temporal water masks should be used in order to exploit the CryoSat-2 dataset to its full potential. In a conservative approach and to optimize data quality one can only retain CryoSat-2 returns over surfaces that are water covered at all times during one year.

		ESA Contract:	1/6287/11/I-NB
		Doc. Title	D5000 Impact Assessment
		Doc. No	Report NCL_CRUCIAL_D5000
		Version No	2
		Date	06.04.17



**Figure 22: Section of the Brahmaputra in the Assam valley showing the Landsat river mask, the CryoSat-2 observations and their mapping to the 1D river model, all for 2013.**

Usually, all individual radar altimetry returns collected over water along one track (i.e. one single overpass of the river) are averaged to produce a single measurement of river water level. This is useful, because it supports outlier detection and makes it possible to estimate a standard error for the retrieved water level. However, especially for north-south or south-north flowing rivers, multiple crossings can occur for a single track or the track may even be aligned with the river course (Figure 23). In such situations, aggregation of individual measurements into groups is still recommended to enable outlier detection and assign a standard error to the water level. We have developed an approach that uses k-means clustering to aggregate the data into a number of groups. The number of groups is determined from the maximum separation of the water returns along one track.

		ESA Contract:	1/6287/11/I-NB
		Doc. Title	D5000 Impact Assessment
		Doc. No	Report NCL_CRUCIAL_D5000
		Version No	2
		Date	06.04.17

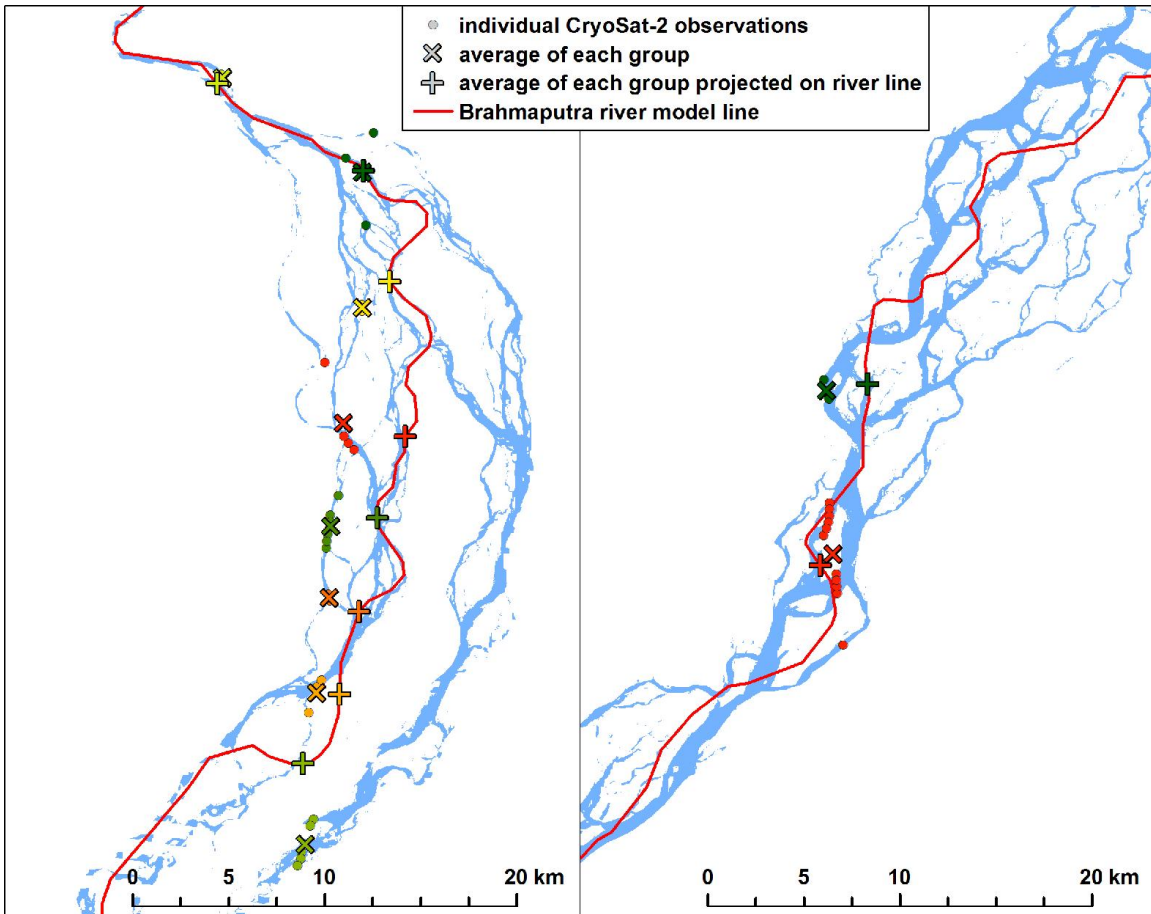




Figure 23: Clustering of individual CryoSat-2 data points from one river crossing based on k-means clustering. The left panel shows a crossing from 09-04-2011, and the right panel from 30-10-2010. Note that the panels are showing different parts of the river, with the 2010 and 2011 river mask respectively.

### 6.3 Calibration of river morphology parameters

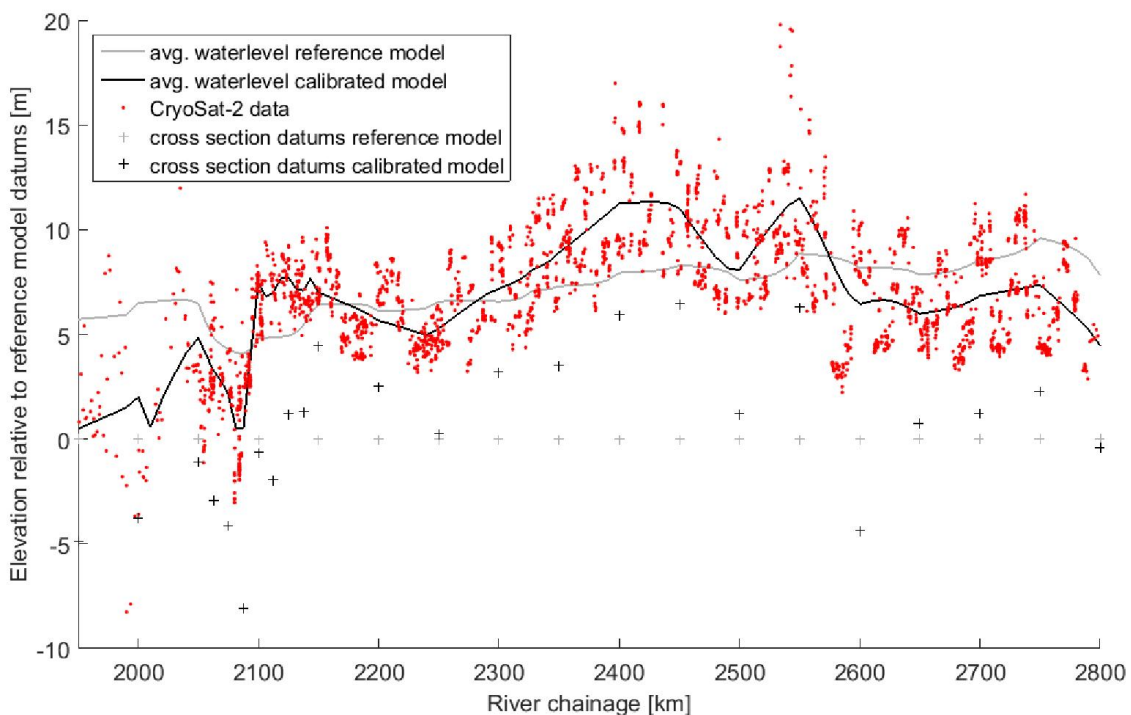
In a one-dimensional representation of a river, river bottom elevation and the shape of the river cross section are key morphology parameters determining the shape and dynamics of the river water table. Assuming that river discharge is known (or predicted with reasonable accuracy by a model), CryoSat-2 observations along the river can be used to calibrate river bottom elevations (Figure 24). This approach has been successfully used for the Assam Valley stretch of the Brahmaputra River in the CRUCIAL project. River bottom elevations obtained with this approach differed significantly from elevations estimated based on the SRTM global DEM. Details are discussed in Schneider et al., 2016b.





		ESA Contract:	1/6287/11/I-NB
		Doc. Title	D5000 Impact Assessment Report
		Doc. No	NCL_CRUCIAL_D5000
		Version No	2
		Date	06.04.17

For a given discharge amplitude, the opening angle of the triangular river cross section determines the corresponding water level amplitude. Water level amplitude can be determined from radar altimetry datasets, most conveniently from virtual station datasets such as Envisat. Such datasets can be used to calibrate the opening angle of river cross sections (Figure 25).

This approach is transferable to other river systems. The representation of river morphology obtained here is expected to produce more realistic and reliable simulations of water levels compared to global DEMs such as SRTM or ASTER GDEM.



**Figure 24: Result of the river bottom elevation calibration for the Assam Valley for the period 2010 to 2013. All levels are shown relative to the reference model's cross section datums based on SRTM DEM.**

		ESA Contract:	1/6287/11/I-NB
		Doc. Title	D5000 Impact Assessment
		Doc. No	Report NCL_CRUCIAL_D5000
		Version No	2
		Date	06.04.17

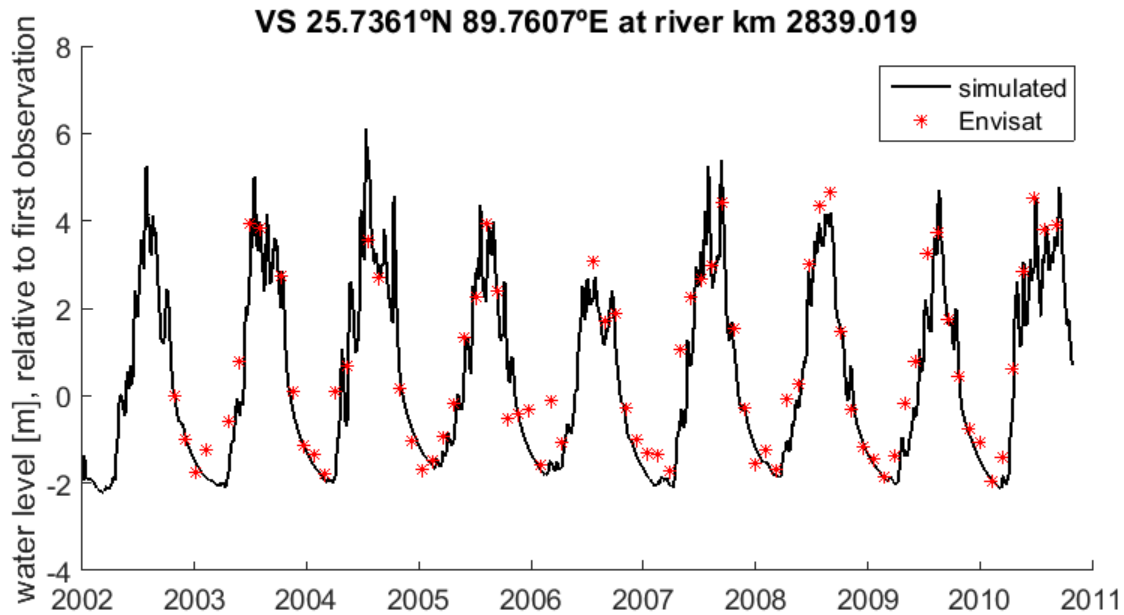


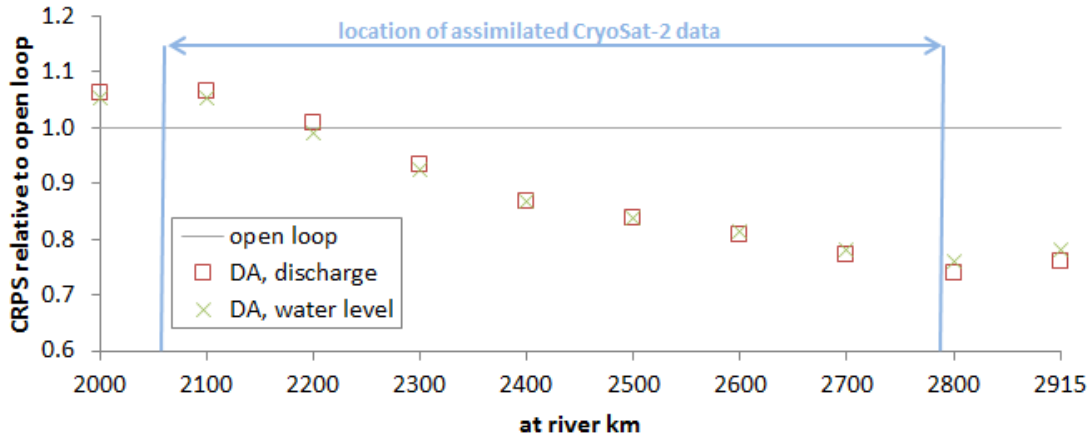


Figure 25: Result of the opening angle calibration for one virtual station. All levels are relative to the water levels at the time of the first Envisat observation. The orbit provides a 35 day repeat cycle.

## 6.4 Synthetic assimilation experiments

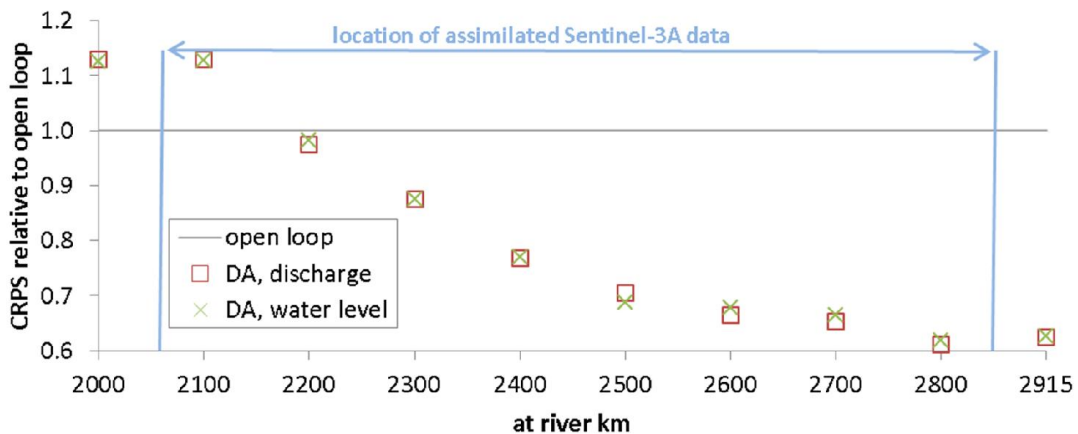
A data assimilation system for 1-dimensional hydrodynamic models has been developed that can be used to assimilate any radar altimetry dataset (repeat orbit, drifting orbit or combined) to a river model (Schneider et al., 2016a). To assess the value of radar altimetry for river modeling and compare different missions and orbit configurations, synthetic data assimilation (DA) experiments are useful. In a synthetic DA experiment, radar altimetry observations are produced synthetically from one specific perturbed model run which is selected as the truth. Synthetic observations are perturbed with random noise and subsequently assimilated to the model. Figure 26 shows the result of such a synthetic DA experiment for the Assam Valley stretch of the Brahmaputra. Performance of the different models is expressed in terms of relative continuous ranked probability score (CRPS). A value of 1 indicates performance equal to the open loop run (i.e. the run without DA), while values below 1 indicate improved performance. It can be seen here that assimilation of CryoSat-2 data for this particular river improves performance by about 20-25% at the downstream end of the stretch. DA of CryoSat-2 can thus improve predictive performance of hydrodynamic models, provided that the model is consistent with the data.

		ESA Contract:	1/6287/11/I-NB
		Doc. Title	D5000 Impact Assessment Report
		Doc. No	NCL_CRUCIAL_D5000
		Version No	2
		Date	06.04.17





**Figure 26: Results of synthetic DA experiment with CryoSat-2 data**

Figure 27 shows the equivalent result for assimilation of Sentinel-3A radar altimetry. The same standard error is assumed for the white noise on the individual measurements as for CryoSat-2. It can be seen that the performance gain from assimilating Sentinel-3A is in our case larger than from CryoSat-2. This can be due to the more regular temporal sampling pattern: Sentinel-3A samples this stretch of the Brahmaputra River in average every 1.1 days, with no gap longer than 3.5 days. CryoSat-2 data however has gaps up to 19 days. Please note that, for the purpose of this synthetic experiment, we assumed that each Sentinel-3A virtual station in the Assam Valley produces usable data for each individual overpass. We know from experience with Envisat, that this may be a very optimistic assumption and real-world performance of Sentinel-3A may therefore be worse than what is shown for this synthetic experiment.



**Figure 27: Results of synthetic DA experiment with Sentinel-3A data**





		ESA Contract:	1/6287/11/I-NB
		Doc. Title	D5000 Impact Assessment
		Doc. No	Report NCL_CRUCIAL_D5000
		Version No	2
		Date	06.04.17

The synthetic data assimilation experiments presented here compare CS-2 and S-3 data value in terms of improvements to model predictive performance under the assumption that river morphology and cross-section geometry are known from in-situ or remote sensing datasets. Using Sentinel-3 data only, it will not be possible to calibrate the water level profile along the entire river as shown in this work for CryoSat-2 data. If Sentinel-3 data is used as part of a multi-mission dataset (including CS2-type data with high spatial resolution), the cross section calibration can be performed using CS2 data prior to assimilation of S3 data. One would have to carefully evaluate and correct for inter-mission biases though.

## 6.5 Assimilation of real CryoSat-2 altimetry

Synthetic DA experiments confirmed the value of CryoSat-2 data for increased predictive performance of hydrodynamic models. This was also confirmed in a run with real CryoSat-2 observations (Figure 28 and Table 8). Improvements are smaller using the real data as compared to the synthetic data (15% vs 25% improvement of CRPS for discharge at Bahadurabad), but are still significant. Reduced performance relative to the synthetic run may indicate that the hydrodynamic model is still not entirely consistent with the CryoSat-2 dataset, due to, for instance, biases in the bottom elevations, or that the model uncertainty description used in the DA runs is insufficient. The system is ready for take-up of other altimetry datasets (e.g. Sentinel-3, AltiKa) to further improve sharpness and reliability of river level and river flow predictions.

CRUCIAL has contributed to the development of hydrodynamic models and forecasting systems for large, ungauged or poorly gauged river basins, with a forward look to Sentinel-3. Multi-mission satellite radar altimetry can be used to inform the river morphology model (cross sections, Manning numbers etc.) and to update the states of the hydrodynamic model (simulated water level and discharge).

		ESA Contract:	1/6287/11/I-NB
		Doc. Title	D5000 Impact Assessment
		Doc. No	Report NCL_CRUCIAL_D5000
		Version No	2
		Date	06.04.17

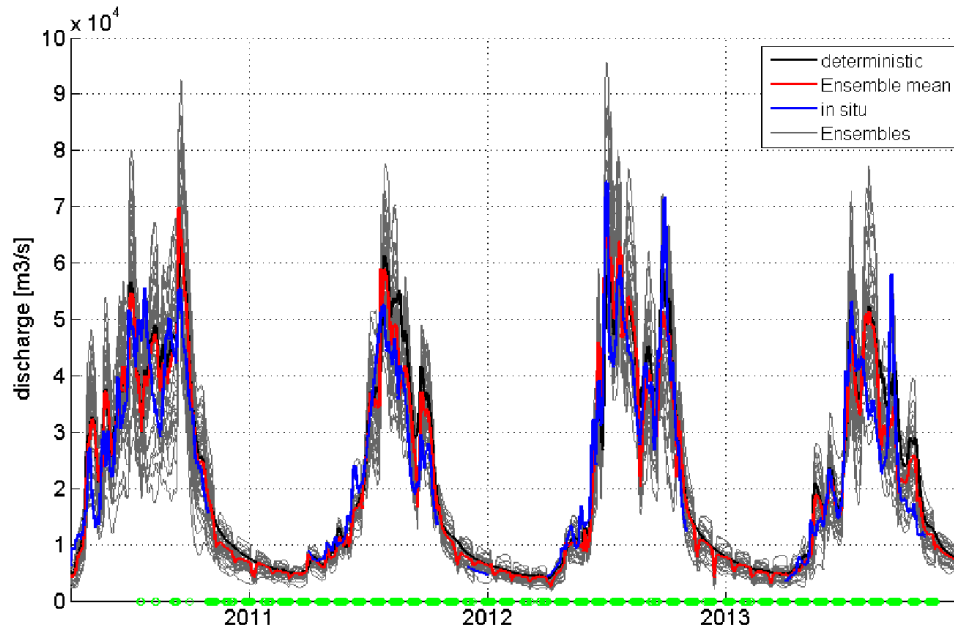




Figure 28: Results of the DA of *real* CryoSat-2 data in terms of *discharge* at Bahadurabad station. The times of observations are marked with green dots on the x-axis.



Table 8: Results of DA experiments using real CryoSat-2 data. Performance is expressed in terms of discharge at Bahadurabad station. Sharpness is given as the width of the 90% confidence intervals

		CRPS [m <sup>3</sup> /s]	sharpness [m <sup>3</sup> /s]
synthetic data	open loop run	3688	15647
	DA, 0.2m obs. error	2778	11500
	DA, 0.4m obs. error	2757	11336
real data	open loop run	4198	14893
	DA	3557	10957

		ESA Contract:	1/6287/11/I-NB
		Doc. Title	D5000 Impact Assessment
		Doc. No	Report NCL_CRUCIAL_D5000
		Version No	2
		Date	06.04.17



## 6.6 Summary and conclusions

Crucial has demonstrated the value of CryoSat-2 data for river analysis and modeling. The mission's drifting orbit makes the CryoSat-2 mission especially interesting and challenging for hydrologists. Using appropriate masking and aggregation techniques, CryoSat-2 can deliver valuable datasets over rivers, which can be used to calibrate river morphology parameters and/or be assimilated to hydrodynamic models. Performance in synthetic DA experiments was comparable to Sentinel-3A and DA experiments with real CryoSat-2 data showed significant improvements of predictive performance. We conclude that CryoSat-2 is a valuable resource for river analysis and modeling, especially due to its spatially dense sampling pattern.

		ESA Contract:	1/6287/11/I-NB
		Doc. Title	D5000 Impact Assessment Report
		Doc. No	NCL_CRUCIAL_D5000
		Version No	2
		Date	06.04.17

## 7. References

- Arsen, A., Crétaux, J-F., and Abarca del Rio, R., 2015. Use of SARAL/AltiKa over Mountainous Lakes, Intercomparison with Envisat Mission, *Marine Geodesy*, 38:sup1, 534-548, DOI: 10.1080/01490419.2014.1002590
- Birkett, C. M., L. A. K. Mertes, T. Dunne, M. H. Costa, and M. J. Jasinski, 2002, Surface water dynamics in the Amazon Basin: Application of satellite radar altimetry, *J. Geophys. Res.*, 107(D20), 8059, doi:10.1029/2001JD000609, 2002.
- Birkinshaw, S. J., O'Donnell, G. M., Moore, P., Kilsby, C. G., Fowler, H. J. and Berry, P. A. M. (2010), Using satellite altimetry data to augment flow estimation techniques on the Mekong River. *Hydrol. Process.*, 24: 3811–3825. doi:10.1002/hyp.7811
- Carroll, M.L., Townshend, J.R., DiMiceli, C.M., Noojipady, P., Sohlberg, R.A., 2009. A new global raster water mask at 250 m resolution. *Int. J. Digit. Earth* 2, 291–308. doi:10.1080/17538940902951401
- Gommenginger, C., Martin-Puig, C., Cotton, P.D., Dinardo, S., and Benveniste, J., 2010, A prototype SAR altimeter retracker to assess the precision of SAR altimetry over the ocean. ESA SeaSAR Workshop 25-29 January 2010
- Kleinherenbrink, M., Ditmar, P.G., Lindenbergh, R.C., 2014. Retracking CryoSat data in the SARIn mode and robust lake level extraction. *Remote Sens. Environ.* 152, 38–50. doi:10.1016/j.rse.2014.05.014
- Nielsen, K., Stenseng, L., Andersen, O.B., Villadsen, H., Knudsen, P., 2015. Validation of CryoSat-2 SAR mode based lake levels. *Remote Sens. Environ.* 171. doi:10.1016/j.rse.2015.10.023
- Schneider, R., Godiksen, P.N., Ridler, M.-E., Villadsen, H., Madsen, H., Bauer-Gottwein, P., 2016a. Combining Envisat type and CryoSat-2 altimetry to inform hydrodynamic models, in: Ouwehand, L. (Ed.), *Proceedings Living Planet Symposium 2016*, ESA Special Publications. European Space Agency, ESA.
- Schneider, R., Nygaard Godiksen, P., Villadsen, H., Madsen, H., Bauer-Gottwein, P., 2016b. Application of CryoSat-2 altimetry data for river analysis and modelling. *Hydrol. Earth Syst. Sci. Discuss.* 1–23. doi:10.5194/hess-2016-243
- Schwatke, C., Dettmering, D., Bosch, W., and Seitz, F. 2015a : DAHITI - an innovative approach for estimating water level time series over inland waters using multi-mission satellite altimetry: , *Hydrol. Earth Syst. Sci.*, 19, 4345-4364, doi:10.5194/hess-19-4345-2015

		ESA Contract:	1/6287/11/I-NB
		Doc. Title	D5000 Impact Assessment
		Doc. No	Report NCL_CRUCIAL_D5000
		Version No	2
		Date	06.04.17

Schwatke C., Dettmering D., Boergens E. 2015b : Potential of SARAL/AltiKa for inland water applications. *Marine Geodesy* (in press), 10.1080/01490419.2015.1008710.

Song C., Ye, Q., Sheng, Y., Gong, T., 2015a, Combined ICESat and CryoSat-2 Altimetry for Accessing Water Level Dynamics of Tibetan Lakes over 2003–2014, *Water*, 7, 4685–4700, doi:10.3390/w7094685

Song, C., Ye, Q., Cheng, X., 2015b. Shifts in water-level variation of Namco in the central Tibetan Plateau from ICESat and CryoSat-2 altimetry and station observations. *Sci. Bull.* 60, 1287–1297. doi:10.1007/s11434-015-0826-8

Westerhoff, R.S., Kleuskens, M.P.H., Winsemius, H.C., Huizinga, H.J., Brakenridge, G.R., Bishop, C., 2013. Automated global water mapping based on wide-swath orbital synthetic-aperture radar. *Hydrol. Earth Syst. Sci.* 17. doi:10.5194/hess-17-651-2013

Wingham, D.J., Francis, C.R., Baker, S., Bouzinac, C., Brockley, D., Cullen, R., de Chateau-Thierry, P., Laxon, S.W., Mallow, U., Mavrocordatos, C., Phalippou, L., Ratier, G., Rey, L., Rostan, F., Viau, P., Wallis, D.W., 2006. CryoSat: A mission to determine the fluctuations in Earth's land and marine ice fields. *Adv. Sp. Res.* 37, 841–871. doi:10.1016/j.asr.2005.07.027